Summer 8-11-2011

Proteomic variations between a Mycoplasma gallisepticum vaccine strain and a virulent field isolate

Rollin Dennard
Georgia State University

PROTEOMIC VARIATIONS BETWEEN A *MYCOPLASMA GALLISEPTICUM* VACCINE STRAIN AND A VIRULENT FIELD ISOLATE

by

ROLLIN DENNARD

Under the Direction of Dr. Georgia Pierce

ABSTRACT

Mollicutes (mycoplasmas) are pathogenic in a wide range of mammals (including humans), reptiles, fish, arthropods, and plants. Of the medically important mollicutes, *Mycoplasma gallisepticum* is of particular relevance to avian agriculture and veterinary science, causing chronic respiratory disease in poultry and turkey. Using two-dimensional electrophoresis based quantitative expression proteomics, the current study investigated the molecular mechanisms behind the phenotypic variability between a *M. gallisepticum* vaccine strain (6/85) and a competitive, virulent field strain (K5234), two strains which were indistinguishable using commonly accepted genetic methods of identification. Twenty-nine proteins showed a significant variation in abundance (fold change > 1.5, p-value < 0.01). Among others, the levels of putative virulence determinants were increased in the virulent K5234, while the levels of several proteins involved with pyruvate metabolism were decreased. It is hoped that the data generated will further the understanding of *M. gallisepticum* virulence determinants and mechanisms of infection, and that this may contribute to the optimization of diagnostic methodologies and control strategies.

INDEX WORDS: *Mycoplasma gallisepticum*, Mollicutes, Poultry vaccine, Expression proteomics, Two-dimensional electrophoresis, DIGE (Difference Gel Electrophoresis)

PROTEOMIC VARIATIONS BETWEEN A *MYCOPLASMA GALLISEPTICUM* VACCINE STRAIN AND A VIRULENT FIELD ISOLATE

by

ROLLIN DENNARD

A Dissertation Submitted in Partial Fulfillment of the Requirement for the Degree of

Doctor of Philosophy

in the Collage of Arts and Sciences

Georgia State University

2011

PROTEOMIC VARIATIONS BETWEEN A *MYCOPLASMA GALLISEPTICUM* VACCINE STRAIN AND A VIRULENT FIIELD ISOLATE

by

ROLLIN DENNARD

Committee Chair: Georgia Pierce

Committee: Sidney Crow

Eric Gilbert

P.C. Tai

Electronic Version Approved:

Office of Graduate Studies

Collage of Arts and Sciences

Georgia State University

August 2011

DEDICATION

To my family

ACKNOWLEDGEMENT

I would like to acknowledge all those who helped along the way.

TABLE OF CONTENTS

ACKNOWLEDGEMENT v

LIST OF TABLES viii

LIST OF FIGURES ix

CHAPTER

1 INTRODUCTION 1

Mollicutes and *Mycoplasma gallisepticum* 1

Expression proteomics 5

Objectives 12

2 EXPERIMENTAL OVERVIEW / MATERIALS AND METHODS 20

Experimental overview 20

Materials and methods 21

3 RESULTS 30

4 DISCUSSION 36

Phase / antigenic variable VlhA 36

Adhesins 41

Energy metabolism and housekeeping enzymes 43

Other proteins of interest 50

Hypothetical proteins 52

Conclusion 54

REFERENCES 61

APPENDIX 69

LIST OF TABLES

Table 1: **Selected sequenced mollicutes** 16

Table 2: **Differential and MS data** 33

LIST OF FIGURES

Figure 1:	**Phylogeny of *Firmicutes***	14
Figure 2:	**Phylogeny of *Mollicutes***	15
Figure 3:	**Pleomorphic *M. gallisepticum***	17
Figure 4:	**DIGE workflow**	18
Figure 5:	**Decyder graphics**	19
Figure 6:	**Cytadherent *M. gallisepticum***	58
Figure 7:	**Pyruvate catabolism in mollicutes**	59
Figure 8:	**$NADP^+$ / thioredoxin system (NTS)**	60

CHAPTER 1

INTRODUCTION

Mollicutes and *Mycoplasma gallisepticum*

Mycoplasmas (specifically *Mycoplasma mycoides*) were first isolated by Nocard and Roux in 1898 (Waites and Talkington, 2004). The designation 'mycoplasma' (mykes, fungi; *plasma*, plasma formed) arose in the 1950's and described the organism's fungus-like growth, a phenotype not actually observed in mycoplasmas other than *M. mycoides*. Since then mycoplasmas have been grouped together in class *Mollicutes* (*mollis*, soft; *cutis*, skin - trivial name, mollicutes or mycoplasmas), which consists of 4 orders, 8 genera, and over 200 species (Johansson and Pettersson, 2002). 16S rRNA phylogenetic data suggest that mollicutes branched off from low GC gram-positive bacteria roughly 600 million years ago (Fig. 1, p. 14), having evolved since then by reductive (or degenerative) evolution, whereby they lost their cell walls and many biosynthetic capabilities (Maniloff, 2002; Razin et al., 1998). To date, over 30 mollicutes have been completely sequenced, with genomes ranging in size from 580 to 1,359 kb (Fig. 2, p. 15; Table 1, p. 16) (Barre et al., 2004). Because of their minute genomes, mollicutes are the subject of intense research efforts aimed at defining the minimal gene compliment required for life, and scientists such as J. Craig Venter are interested in using this data to synthesize life *in vitro* (Glass et al., 2006).

Mollicutes are highly pleomorphic, exhibiting spherical (0.3 – 0.8µm in diameter), pear shaped, flask shaped, and filamentous cell morphologies. Colonies are typically fried egg shaped (Razin et al., 1998). Structurally, "*Mollicutes* are characterized by the complete lack of a cell

wall and the presence of an internal cytoskeleton" (Wolf et al., 2004). Cell growth is unaffected by cell wall synthesis-inhibiting antibiotics, and chemical analysis confirms the absence of peptidoglycan, muramic acid, and diaminopimelic acid in mollicutes (Madigan et al., 2006). Genetic studies show that mollicutes do not have the genes needed for the biosynthesis of these cell wall components (Waites and Talkington, 2004).

Mollicutes are not as sensitive to osmotic shock as are typical protoplasts. This is due to the presence of sterols, which are rigid and planar, in their cell membranes (unique among bacteria). Some mollicutes possess lipoglycans which add to the stabilization of their membranes (Madigan et al., 2006). The plasma membranes are also supported by an internal cytoskeleton that is involved in modulating cell shape, cell division, localization of adhesins, and motility (Balish and Krause, 2002; Razin et al., 1998).

While some mollicutes are strictly respiratory, most are facultative anaerobes (Madigan et al., 2006). Glucose is metabolized by glycolysis or an incomplete pentose phosphate shunt. Most non-fermentative and some fermentative mollicutes possess an arginine dehydrolysis pathway. It is thought that substrate level phosphorylation during these catabolic pathways accounts for most of the ATP production in mollicutes. Mollicutes lack TCA cycles, have truncated electron transport chains (flavin terminated, no quinones or cytochromes), and are incapable of oxidative phosphorylation (Pollock et al., 1997; Razin et al., 1998). Anabolism in mollicutes relies heavily on the uptake of many biosynthetic precursors, including amino acids, purines, pyrimidines, and cholesterols (Madigan, 2006). As Shmuel Razin states, "metabolic activities appear to be associated primarily with energy production rather than providing substrate for biosynthetic pathways" (Razin et al., 1998).

Mollicutes have never been isolated as free-living entities in nature. Their limited biosynthetic capabilities obligate them to symbiotic, commensal, or parasitic lifestyles. Parasitic mollicutes are pathogenic in a wide range of mammals, reptiles, fish, arthropods, and plants (Table 1, p. 16). Animal mycoplasmas colonize the epithelial cells of mucosal surfaces, such as respiratory and urogenital tracts, alimentary canals, mammary glands, and joints. In humans, mycoplasmas are the primary agents of urethritis and respiratory diseases, and two strains have been implicated as cofactors in HIV infections (Barre et al., 2004; Razin et al., 1998).

Despite their medical relevance, little is known about the pathogenicity of mollicutes. Infections are typically chronic, as mollicutes are able to subvert host immune responses by cellular invasion, survival within phagocytic and non-phagocytic cells, and the generation of phenotypic variants (Rottom, 2003). Potent toxins have not been identified, but mechanisms of pathogenicity may include competition for biosynthetic precursors, damage induced by cytadherence, damage induced by fusion, oxidative damage due to mildly toxic metabolic byproducts such as hydrogen peroxide and superoxide radicals, cytopathic effects of hydrolytic enzymes, and indirect damage resulting from the host's inflammatory and cellular responses (Bradbury, 2005). Antimicrobial therapies have been only partially successful (Razin et al., 1998).

Of the medically important mollicutes, *M. gallisepticum* is of particular relevance to avian agriculture and veterinary science, contributing to chronic respiratory disease in poultry and turkeys. *Mycoplasma gallisepticum* is one of the motile and predominately flask shaped mollicutes (Fig. 3, p.17). The flask shape is conferred by a terminal tip organelle, which is involved in attachment, motility, and cell division. The organism spreads through flocks laterally by aerosol exposure and vertically by egg transmission and then colonizes respiratory tracts via

attachment epithelial tissue (Papazisi et al., 2003). M*ycoplasma gallisepticum* has also been isolated from the reproductive organs, brains, eyes, and joints of several avian species. Dissemination within the host is thought to be aided by the organism's ability to adhere to, penetrate, and survive within the host's red blood cells. Complications (decreased egg production and increased vaccination and medication cost) caused by *M. gallisepticum* infections have a severe negative economic impact on both the poultry and turkey industries (Papazisi et al., 2003). Despite a worldwide impact, mechanisms of *M. gallisepticum* pathogenicity are not well understood. Outbreaks are difficult to control, often necessitating eradication of diseased populations (Papazisi et al., 2003).

Currently, there are three commercial *M. gallisepticum* live attenuated vaccine (LAV) strains available in the United States: F-strain, ts-11, and 6/85. Strain 6/85 does not persist well in birds but has low virulence and low potential for transmission from vaccinated to non-vaccinated chickens (Evans and Hafez, 1992). In 2002, a report was published that described a 6/85-like strain found within and near a flock of chickens that had been vaccinated with 6/85 (Throne-Steinlage et al., 2003). Increased mortality and sinus swelling were observed in both vaccinated and unvaccinated birds. Tracheal cultures yielded a strain that was indistinguishable from 6/85 by random amplified polymorphic DNA (RAPD) and gene-targeted sequencing (GTS) of four genes (*gapA*, *LP*, *mgc2*, and *pvpA*). However, the field isolate, designated K5234, differed significantly from the vaccine strain in field trials. The field isolate produced a much stronger antibiotic response and colonized the trachea much more effectively than did the vaccine strain (Throne-Steinlage et al., 2003). Thus, while the two strains were indistinguishable RAPD and GTS, the 6/85-like strain had the interesting phenotypes of increased antibiotic response, colonization, and persistence in experimental chickens.

Using two-dimensional electrophoresis based quantitative expression proteomics, the current study investigated the proteomic variations between strains 6/85 and K5234 in order to develop a more comprehensive understanding of the molecular basis of *M. gallisepticum* virulence and attenuation and thereby contribute to the optimization of control strategies.

Expression Proteomics

While the amount of genetic information is staggering (117 billion base pairs currently in Genbank), there is a general acceptance that DNA sequences alone are inadequate when the goal is to develop a global, real time understanding of biological systems (Beranova-Giorgianni, 2003). As genes may or may not be expressed, an organism's genome can be thought of as a potential or a "blueprint" (Simpson, 2003). To a certain extent, mRNA also indicates a potential physiological state; numerous modifications can take place above the level of transcription, including post-transcriptional and translational modifications, proteolysis, protein degradation, and compartmentalization (Graves and Haystead, 2002). Various studies have also revealed poor correlations between mRNA levels and their corresponding protein levels (Ghaemmaghami et al., 2003; Graves and Haystead, 2002; Ideker et al., 2001). On the other hand, proteins can be thought of as actuality; they "mediate the greater part of cellular activities" and are directly related to a cell's real time physiological state (Tannu and Hemby, 2006). As Richard J. Simpson writes, proteins can be viewed as "bridges between genotype and phenotype" (Simpson, 2003).

The term proteome was originally defined as "the complete set of proteins that is expressed, and modified following expression, by the entire genome in the lifetime of a cell" (Wilkens et al., 1996). Currently, the most common definition of proteome is "the entire

complement of proteins expressed by a cell at any one time," a definition that reflects the dynamic nature of protein expression (Anon., 1999). The goal of most non-targeted proteomic research is to gain a more global understanding of biological systems by analyzing as many proteins as possible. The global data can then be used as a platform for more targeted studies and also be integrated with other "omic" (genomic, transciptomic, and metabolomics) data (Graves and Haystead, 2002; Simpson, 2003). This approach forms the core of systems biology, a discipline "which aim[s] at a systems level understanding of genetic or metabolic pathways by investigation of interrelationships…and interactions…of genes proteins, and metabolites" (Selinger, 2003; Wolkenhauer, 2001).

Proteomics can be divided into four broad areas: bioinformatic based proteomics, structural proteomics, functional proteomics, and expression proteomics. Bioinformatic based proteomics takes advantage of computational tools and resources to conduct *in silico* experiments (Westermeier and Naven, 2002). The goal of structural proteomics is the analysis of protein complexes. Functional proteomics is a general term used to describe more specific, directed studies. Expression proteomics (or comparative protein profiling) is the quantitative study of protein levels between two systems that differ by some variable (Graves and Haystead, 2002).

Two dimensional electrophoresis (2DE) / mass spectrometry (MS) based expression proteomics is of particular value to the microbial cell physiologists interested in investigating molecular mechanisms involved with phenotypic variations. By identifying proteins that vary in abundance between two samples, it is possible to link certain proteins to observed phenotypic variations, leading to the elucidation of molecular mechanisms responsible for processes of

interest. For applied microbiologists, this increases the potential targets for affecting cellular processes.

Two-dimensional electrophoresis was developed by O'Farrell in 1975 (O'Farrel, 1997). The technique is used to resolves complex mixtures of proteins by separating the proteins according to two independent characteristics: isoelectric point (pI) and molecular weight (MW). In the first dimension, proteins are separated according to their pI using isoelectric focusing (IEF). In the second dimension, proteins are separated according to their MW using sodium dodecyl sulphate polyacrylamide gel electrophoresis (SDS-PAGE). After the proteins are separated, variations in protein levels between the two samples are determined using image analysis and quantification software. Proteins of interest are then characterized by MS.

Protein separation by 2DE can be broken down into four stages: sample preparation, IEF, SDS-PAGE, and image analysis. As one scientist has noted, "[s]ample treatment is the key to adequate [2DE] results" (Westermeier and Naven, 2002). Typically, cells are lysed directly into a solubilization buffer that is compatible with IEF and will ensure high resolution. The buffer must achieve the following tasks: convert all proteins into single conformations, cancel different oxidation steps, disrupt protein aggregates, prevent protein modification, and disrupt hydrogen and disulphide bonds. Additionally, the solubilization buffer must satisfy the constraints of IEF, namely that conductive substances are kept to a minimum (Shaw and Riederer, 2003). Standard solubilization buffers contain urea, a nonionic or zwitterionic detergent, a reductant, and carrier ampholytes. Urea denatures proteins by disrupting hydrogen bonds and hydrophobic interactions, converting proteins into single conformations. Nonionic detergents, such as NP-40 and Triton X-100, and zwitterionic detergents, like 3-[3-(cholamidopropyl)dimethylammonio]-1-propane sulfonate (CHAPS), prevent hydrophobic interactions and loss of protein due to aggregation and

precipitation. Reductants cleave intra-and intermolecular disulphide bonds between cysteine residues, converting them to sulfhydral groups. Carrier ampholytes minimize protein aggregation due to charge-charge interactions and scavenge isocyanate, a urea derivative which is capable of modifying proteins and thereby generating artificial protein spots. (Simpson, 2003; Westermeier and Naven, 2002).

Once the proteins have been solubilized, they are applied directly to the first dimension IEF gel. Isoelectric focusing takes advantage of the amphoteric nature of proteins. The net charge of a protein is dependent on the pH of its environment. The pH of the environment where the net charge of a protein is zero is called its isoelectric point (pI). If the pH of the environment is above a protein's pI, then the protein will have a net negative charge. If the pH of the environment is below a protein's pI, then the protein will have a net positive charge. When placed in a pH gradient with a current, proteins will migrate toward the electrode opposite their net charge, negatively charged proteins migrating toward the anode and positively charged proteins migrating toward the cathode. Proteins will stop (focus) when the pH of the gradient equals their pI, and they have no net charge (Westermeier and Naven, 2002).

Traditionally, IEF gel gradients were created with mixtures of carrier ampholytes, small amphoteric buffers with isoelectric points over a broad range and high buffering capacities near their pI. The ampholytes were mixed with low percent (so that there was no sieve effect) acrylamide monomer, and a current was applied. The buffers migrated accordingly, forming a pH gradient. This method was problematic for several reasons. During electrophoresis, the gradients were unstable and would drift. Additionally, there was significant batch-to-batch variability and gradients could not be extended above a pH of 7.5. Also, proteins could act as ampholytes and modify the gradients, making the gel gradients sample specific (Simpson, 2003).

Many of these problems were overcome with the development of immobilized pH gradients (IPG) by Bjellqvist and coworkers (Bjellqvist et al., 1982). Immobilized pH gradients use acrylamide derivatives instead of carrier ampholytes. The derivatives have carboxylic acid and tertiary amino acid reactive groups. Typically, glycerol is added to a solution of the acidic acrylamide buffer and linearly mixed with a solution of basic acrylamide buffer. Upon polymerization, the reactive groups covalently bind the gel matrix. The gels are bound to a support film, dried down, and then cut into strips. Because the gradient is bound to the gel matrix, it is stable, and batch-to-batch variation is minimized. Immobilized pH gradient gels also have a much higher loading capacity than traditional carrier ampholyte gels (Simpson, 2003).

After the first dimension and before the second dimension, the proteins in IEF gels need to react completely with SDS, be re-reduced, and alkylated. This is achieved by equilibrating the strips twice in a buffer containing SDS, urea, and glycerol. During the first equilibration, dithiothreitol (DTT) is added to the equilibration buffer to ensure that all proteins are reduced. Iodoacetamide is added to the second equilibration buffer to alkylate sulfhydral group, preventing re-oxidation. Iodoacetamide also scavenges excess DTT (which can cause streaking) and aids MS analysis (Gorg et al., 2000).

Isoelectric focusing gels are applied directly onto the tops of SDS-PAGE gels. Sodium dodecyl sulphate polyacrylamide gel electrophoresis separates proteins according to their MW. Gels are composed of polymerized acrylamide and N,N’methylenebisacrylamide. During electrophoresis, negatively charged SDS-protein complexes migrate toward the anode, with the gel acting as a porous sieve. The migration distance of a protein is logarithmically related to its MW. Low MW proteins will migrate further than high MW proteins (Westermeier, 2001).

Theoretically, combining IEF and SDS-PAGE could separate up to 10,000 proteins. However, only up to 2,000 proteins are routinely separated in laboratories (Gorg et al., 2004).

Once a protein extract has been separated by 2DE, MS is typically used to characterize the proteins of interest. Mass spectrometry measures the relative MW of molecules by converting them to gas phase ions and separating the ions according to their mass:charge (m/z) ratio. Most MS instruments contain three modules: the ionization source, the mass analyzer, and the detector. The ionization source converts the molecules into gaseous ions by adding protons or subtracting electrons. The mass analyzer uses a magnetic or electric field to propel the ions toward a detector which monitors the magnitude of the current from the ions as they reach the end of the mass analyzer (Henzel et al., 2003).

Of the multiple MS configurations used in protein science, matrix assisted laser desorption ionization–time of flight (MALDI-TOF) is one of the most simple, robust, and amendable to high throughput (Aebersold, 2003). Typically, the sample is digested with trypsin, and the peptide digest is co-crystallized with a matrix, which is a small organic molecule that absorbs specific wavelengths of light. The dried sample is pulsed with UV light and energy is transferred from the matrix to the analyte, causing desorption and ionization. The initial velocity of an ion is dependent upon its mass, and an ion's time of flight in the analyzer is proportional to the square root of its m/z ratio. Smaller molecules will reach the detector before larger molecules. The MW of molecules in a complex mixture can be determined by comparing their time of flight to that of a standard (Westermeier and Naven, 2002). Ultimately, a spectrum is generated that contains the MW of each peptide fragments in the protein digest.

The MALDI-TOF can also be configured for tandem MS or MALDI-TOF/TOF. With this configuration, two TOF analyzers are split by a collision cell. In the first analyzer, specific

ions are selected and then energetically fragmented by collision-induced dissociation (CID) in the collision cell. The fragments are then separated by the second TOF analyzer (Westermeier and Naven, 2002). Matrix assisted laser desorption ionization–time of flight/time of flight produces two types of data. The first type is called peptide mass fingerprints (PMF), which is a spectrum generated from the MWs of the unfragmented tryptic peptide digests (MS data). A protein is identified by comparing its experimental spectrum to those of theoretically digested proteins in a database. The second type of data is sequence information deduced from the fragmented peptides (MS/MS data). Usually, two or more fragment sequences are enough to identify a protein (Henzel et al., 2003). The two types of data are used separately or in conjunction to characterize a protein.

The current study used 2DE / MALDI-TOF/TOF MS in conjunction with difference gel electrophoresis (DIGE) technology to quantify proteomic variations between two organisms. Difference gel electrophoresis employs a set of three cyanine dyes (Unlu et al., 1997) and computer software (Decyder) designed exclusively for use with these dyes. The three fluorescent dyes (Cy™2, Cy™3, and Cy™5; Piscataway, NJ), which bind lysine, are matched for charge and mass and are spectrally distinct. A protein labeled with each of the fluors will migrate to the same position on a gel (co-migration). Images can be generated for each of the Cy™-labeled samples, and differential data is generated by comparing the pixel intensities of the fluors (Minden et al., 09; Tonge et al., 2001). Typically, control and variant samples are labeled with either Cy™3 or Cy™5. In practice, reverse-labeling may be employed to cancel any protein specific variation in labeling between the two dyes. A standard sample (internal standard) containing equal amounts of protein from each sample in the experiment is labeled with Cy™2. After the labeling reaction, the three Cy™- labeled samples are mixed together (multiplexed) and

then separated by 2DE (Fig. 4, p. 18; Fig. 5, p. 19). Because each dye has different excitation /emission requirements, one image for each of the multiplexed samples can be generated (Alban et al., 2003).

The inclusion of an internal standard offers several advantages. First, a direct ratio of each protein spot to its representative internal standard on the same gel can be derived (intra-gel analysis). This ratio can then be compared with the ratios of the same spot on different gels (inter-gel analysis), allowing the detection of small changes above experimental and biological variation to be detected with high statistical significance (DeCyder, Version 5.0). The internal standard also facilitates gel matching. With conventional systems, different samples from different gels have to be matched. With the DIGE system, the internal sample is the same sample on each gel, making matching easier and more accurate (DeCyder, Version 5.0).

Objectives

The goal of the current project was to identify proteomic variation between a *M. gallisepticum* vaccine strain (6/85) and a closely related virulent, field isolate (K5234) which varied in phenotypes of medical relevance. The project was deemed well suited for 2DE / MALDI-TOF/TOF MS based proteomics for several reasons. In order to characterize a protein using MALDI-TOF/TOF MS, the protein's gene has to have been sequenced. The *M. gallisepticum* prototype strain, R_{low}, has been completely sequenced. It contains a 1,012,80 bp genome with 784 genes, 469 of which have been functionalized (Papazisi et al., 2003; Szczepanek et al., 2010). Because of *M. gallisepticum's* small genome, 2DE would provide a high percent coverage of the *M. gallisepticum* proteome. Also, because the two strains being compared had very similar genomes (as determined in the preliminary evaluations), the data set

was predicted to be manageable, enabling some of the protein level variations to be linked to the observed phenotypic variations between the two strains. The objectives of the project were first to identify proteins that varied in abundance between 6/85 and K5234 using 2DE, and then to characterize these proteins by MALDI-TOF/TOF MS. It was hypothesized that some of the identified proteins could be implicated in the increased colonization and virulence of K5234, thereby shedding light on the mechanisms employed by *M. gallisepticum* during the infection of its host.

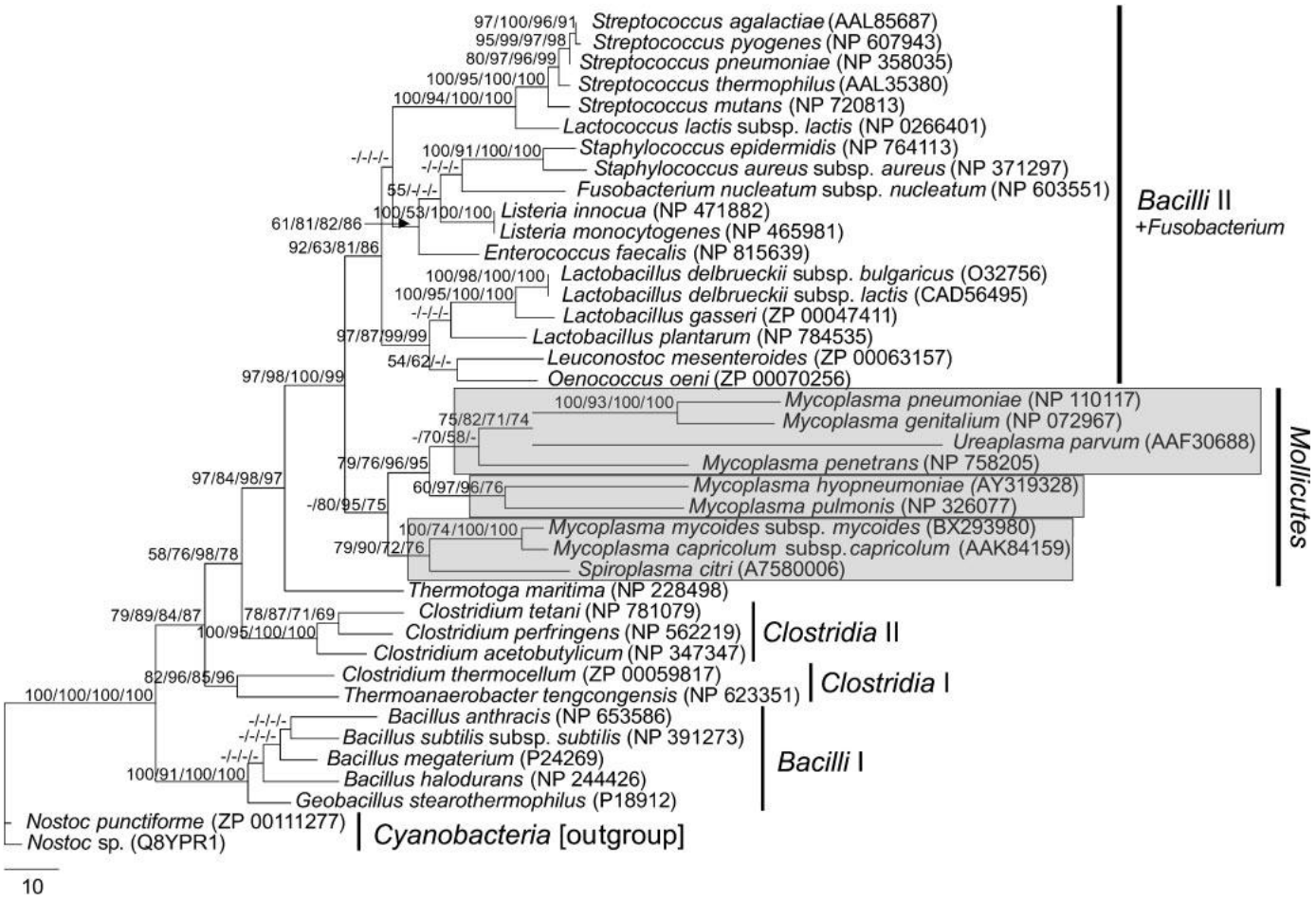

Fig. 1. Phylogeny of *Firmicutes*. Mollicutes branched off from the low GC gram-positive bacteria (Wolf et al., 2004).

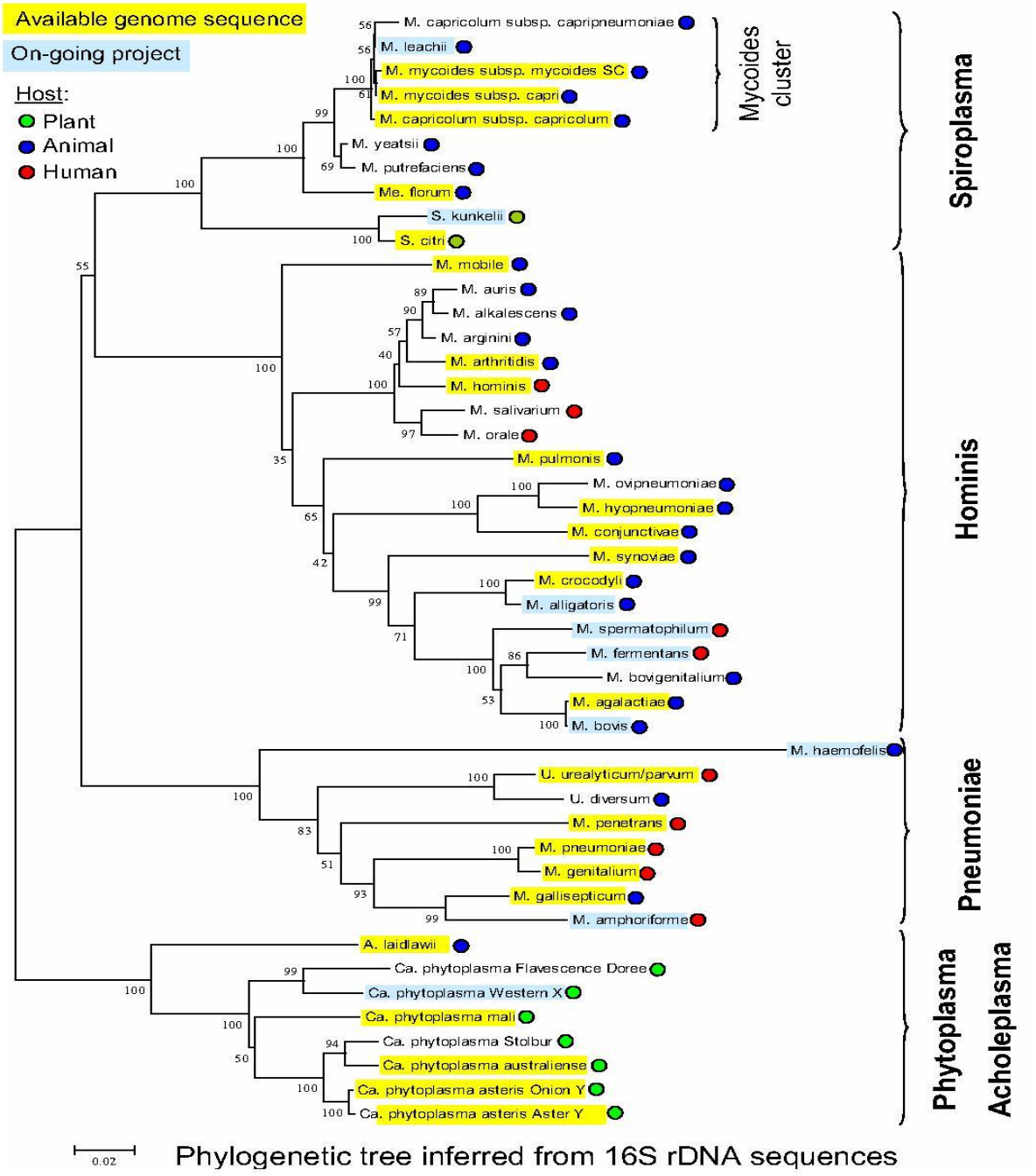

Fig. 2. Phylogeny of mollicutes. *M. gallisepticum* is in the same phylogenetic cluster as *M. pneumoniae* and *M. genitalium*, the two most well-studied mollicutes (Barre et al., 2004).

Table 1. Selected sequenced mollicutes. Species listed in order of increasing genomic size (Barre et al., 2004).

Organism	Associated disease (host)	kb	Genes
M. genitalium	Urogenital or respiratory tract infection (human)	580	484
Candidatus AY-WB	Aster yellows / witches'-broom (plant)	707	671
Ureaplasma urealyticum	Septicaemia / meningitis / pneumaonia (human)	752	614
M. mobile	(fish)	777	667
Mesoplasma flurum	(animal)	793	683
M. synoviae	Chronic respiratory disease / synovitis (poultry)	799	672
M. pneumonia	Atypical pneumonia (human)	816	689
Candidatus asteris OY	Onion yellow disease (plant)	861	754
M. agalactiae	Contagious aglactia (small ruminant)	877	752
M. hypneumoniae 232	Pleuropneumonia (swine)	691	691
M. hypneumoniae J	Enzootic pneumonia (swine)	897	665
M. hypneumoniae 7448	Enzootic pneumonia (swine)	920	663
M. pulmonis	Respiratory infection (murine)	964	782
M. gallisepticum	Chronic respiratory disease (poultry and turkey)	996	726
M. capricolum	Severe arthritis / septicemia (animal)	1010	827
M. mycoides	Pleuropneumonia (cattle)	1212	1016
M. penetrans	Urogenital and respiratory tract infections (human)	1359	1037

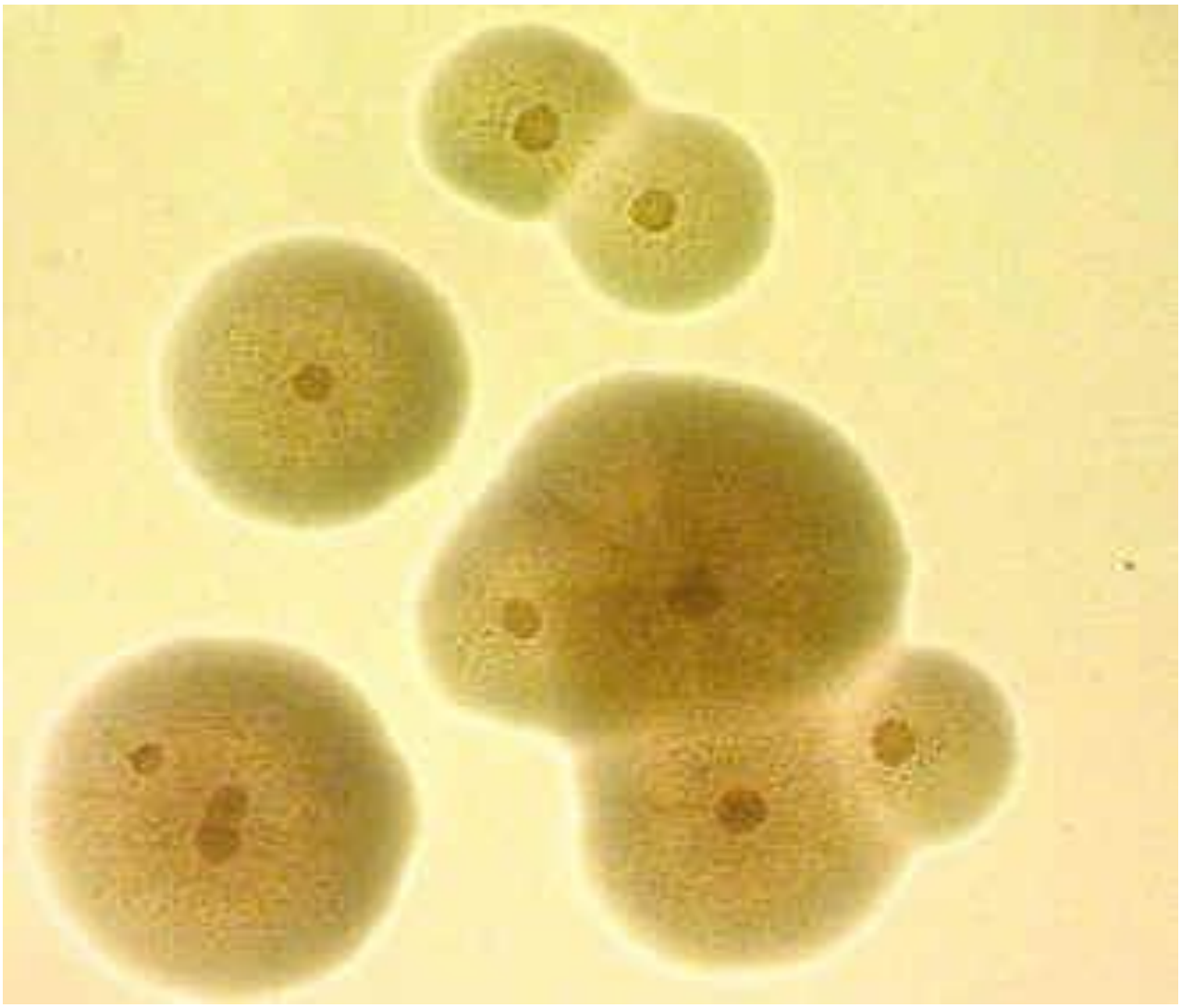

Fig. 3. *M. gallisepticum* cell morphology (Barre et al., 2004).

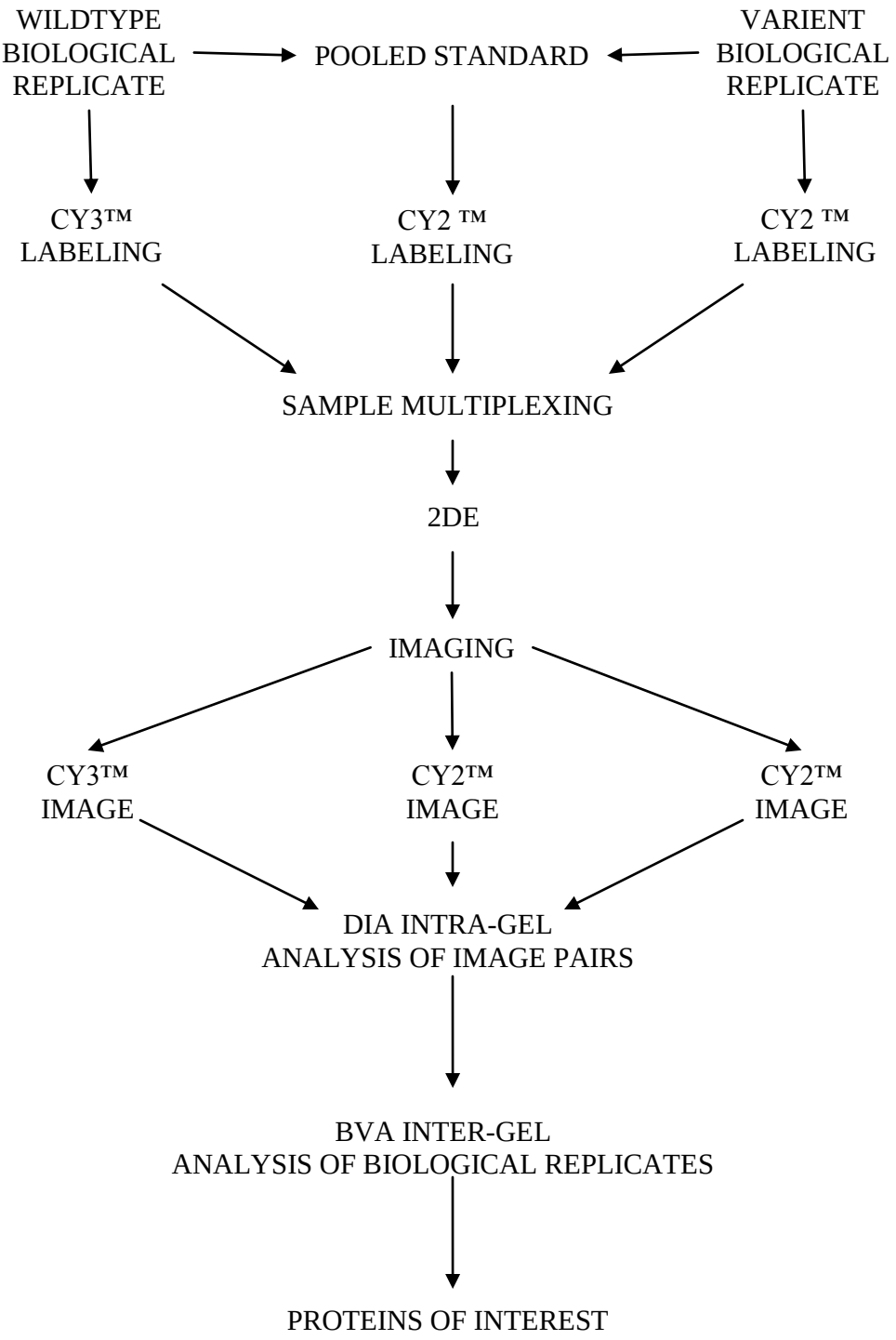

Fig. 4. DIGE workflow. Figure does not reflect reverse-labeling**.**

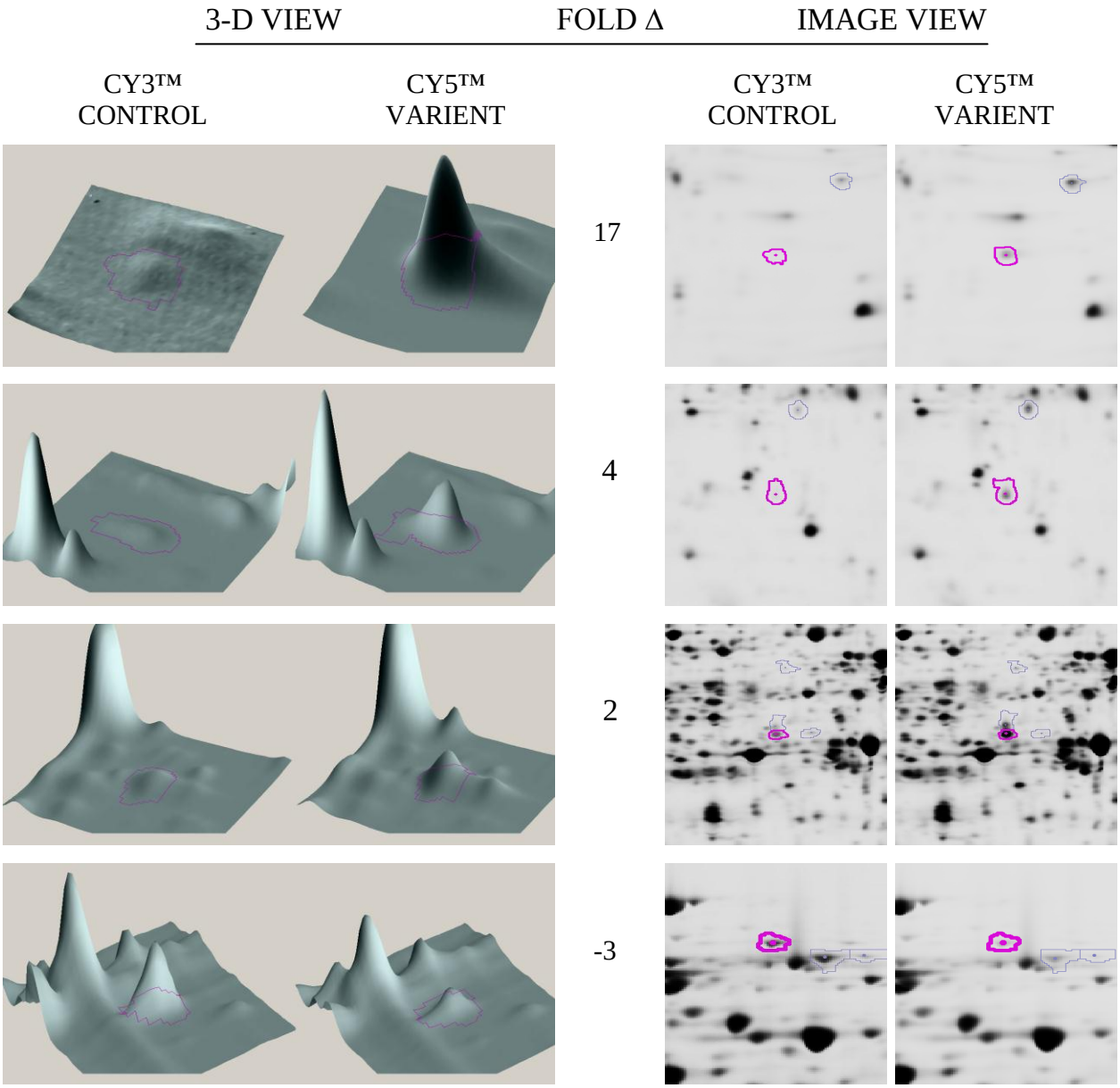

Fig. 5. DeCyder graphics. 3-D view is a normalized volumetric depiction of variations in pixel intensities between control and variant samples.

CHAPTER 2

EXPERIMENTAL OVERVIEW AND MATERIALS AND METHODS

Experimental overview

Mycoplasma gallisepticum 6/85 and K5234 were grown under identical conditions and harvested during mid-exponential phase. Cells were mechanically disrupted and a crude, soluble protein extract was prepared. Protein extracts from four biological replicates of each strain were individually labeled with Cy™ dyes. According to best laboratory practice, reverse-labeling (dye swaps or flip dye) was employed. Half of the 6/85 extracts were labeled with Cy™2 and half were labeled with Cy™5. K5234 extracts were labeled similarly. A standard sample was prepared by mixing equal amounts of protein from each of the eight extracts. The standard was labeled with Cy™2. The samples were multiplexed by combining one Cy™3 sample, one Cy™5, and one Cy™2 standard sample. The four multiplexed samples, along with an unlabeled standard sample (a preparative load) were separated by 2-DE, using both 3-7NL and 7-11 IEF strips. Variations in protein levels between the two cell types were determined using Decyder™ Differential Analysis Software, Version 5.0. Proteins that varied in abundance above 1.5 fold or below -1.5 fold and with p-values below 0.01 were located on a preparative gel. Proteins of interest were picked and then characterized by MALDI-TOF/TOF MS.

Materials and Methods

Except where otherwise indicated, all reagents were purchased from Sigma-Aldrich. Samples for both 4-7NL and 7-11 gel sets were derived from the same protein extracts. Identical methods and conditions were used for both gel sets.

Cell growth. *Mycoplasma gallisepticum* strains 6/85 and K5234 were cultivated in Frey's medium (Throne-Steinlage et al., 2003) at 37°C. Starter cultures (10 ml Frey's medium) were inoculated with 100 µl of glycerol stock and incubated for 14 h. For each strain, 1.25 ml of the starter cultures were used to inoculate each of four 1-L flasks containing 450 ml of media. The cultures were incubated at 37°C and 100 rpm in a NBS Gyratory shaker (New Brunswick, NJ). Cell growth was monitored by plate counts and $OD_{600/640}$. According to previously established growth curves, the cultures were harvested by centrifugation (3,000 x g for 20 min at 4°C) during mid-exponential phase (18 h). The cell pellets were washed three times in 10 mM tris(hydroxymethyl)aminomethane chloride (TrisCl), pH 8.8, and 5 mM magnesium acetate. The pellets were stored at -70°C.

Preparation of lyses buffer. Twelve grams of urea and 4.5 g of thiourea were dissolved in 12 ml of ddH_2O. The volume was made up to 25 ml with ddH_2O, giving a solution of 8 M urea and 2.3 M thiourea. To this solution, 250 mg of PlusOne™ Amberlite IRN-150L (GE Healthcare) were added, and the suspension was stirred for 1 h on a magnetic stirrer and then filtered through a 0.45-µm filter (Millipore). The following components were added to 13.2 ml of the de-ionized urea / thiourea solution: 450 µl of 1 M Tris, 150 µl of nuclease mix (GE Healthcare), 300 µl of protease inhibitor mix (GE Healthcare), and 600 mg of 3-[(3-Cholamidopropyl)dimethylammonio]-1-propanesulfonate (CHAPS). The pH was adjusted to 8.6 with concentrated hydrochloric acid. The lyses buffer was diluted to 15 ml with ddH_2O, making

the final concentration: 30 mM Tris, 7 M urea, 2 M thiourea, 4% CHAPS, 1% nuclease mix (GE Healthcare), and 2% protease mix (GE Healthcare). The lyses buffer was aliquoted in 1ml-cryovials and stored at -70ºC for a maximum of 3 months.

Soluble protein extract. Nine hundred milliliters of lyses buffer were added to each cell pellet. The samples were vortexed vigorously and then incubated on ice for 10 min. The cell slurries were transferred to 50 ml glass centrifuge tubes and sonicated (Sonicator® Ultrasonic Processor XL, Misonix) on ice six times (15 s on followed by 15 s off) using a 50% duty cycle. Following sonication, the samples were incubated at room temperature for 1 h and then clarified by centrifugation (40,000 x g for 1 h at 7°C). Protein concentrations were determined using a 2-D Quant Kit (GE Healthcare). The clarified lysates were stored at -70°C until labeling.

Minimal CyDye™ labeling. The 6/85 (control) and K5234 (variant) samples were diluted with lyses buffer to a protein concentration of 5 mg/ml in a volume of 75 µl. A pooled sample, containing equal amounts of protein from each sample, was generated by mixing together 55 µl of each of the eight samples. For the preparative gels, 40 µl (200 µg) of the standard were transferred to a reaction tube. For the analytical gels, 10 µl (50 µg) of each of the control/variants samples were transferred to separate reaction tubes.

CyDye™ DIGE fluors (GE Healthcare) were reconstituted according to the manufacturer's instructions. Un-opened 10 mM dyes were thawed on ice for 5 min. Ten microliters of N,N-dimethylformanide (DMF) were added to each dye, making the final concentration 1 mM. The dyes stocks were vortexed vigorously for 30 s, centrifuged briefly, and stored at -20°C.

The labeling reactions were carried out on ice and protected from light according to the manufacturer's protocol. Working dye solutions consisted of 3 µl of the 1 mM dye stocks and

4.5 µl of DMF, giving a final dye concentration of 400 µM. The control and variant biological replicates were reverse-labeled. Half of the controls samples were labeled with 1 µl of Cy™3 (400pmol), and the other half were labeled with 1 µl of Cy™5. The variant samples were labeled similarly. Four microliters of Cy™2 were added to reaction tubes which contained 40 ul of the pooled sample. The samples were incubated for 30 min, and then the reactions were quenched with 1 µl of 10 mM lysine. The samples were incubated for an additional 10 min and then stored at -70°C.

Sample reduction. Multiplexed sample sets for each of four analytical gels were made by marrying a Cy™3, Cy™5, and Cy™2 labeled sample (50 µg 6/85, 50 µg K3234, and 50 µg standard - a total of 150 µg of protein). Equal volumes of 2X sample buffer - 7 M urea, 2 M thiourea, 4% CHAPS, 10 mM dithiothreitol (DTT), and 2% 3-11 non-linear ampholytes (GE Healthcare) - were added to each of the multiplexed samples. The preparative gel sample loads were reduced by adding equal volumes of 2X sample buffer to 200 µg of the pooled samples. The samples were vortexed and then incubated on ice for 30 min protected from light.

Two-dimensional electrophoresis. The proteins were separated by 2DE according to the methods of O'Farrel, as modified by Gorg et al., and described by Westermeier (O'Farrel, 1975; Gorg et al., 2000; Westermeier and Naven, 2002). Using a reswelling tray (GE Healthcare), IPG strips (GE Healthcare) were rehydrated for 24 h in Destreak™ Rehydration Solution (GE Healthcare). For both 4-7NL and 7-11 IPGstrips, the rehydration solution was supplemented with 1.0% 3-11NL ampholytes (GE Healthcare). The rehydrated strips were transferred to cup loading strip holders (GE Healthcare), oriented so that the plastic backing was down and the gel face up. The strips were covered with 4.4 ml of mineral oil. Electrode pads moistened with 150 ul of ddH_2O were placed at the ends of the gels. Protein samples were loaded at the acidic end of the

strips via sample cups. The strips were focused for ~ 50, 000 volt/h (4 h at 300 V, 6 h gradient from 300 V to 1,000 V, 3 h gradient from 1,000 V to 8,000 V, and 4 h at 8,000 V) using an Ettan™ IPGphor™ Isoelectric Focusing System (GE Healthcare). The focused strips were stored in plastic tubes at -70°C.

Casting second dimension SDS-PAGE gels. Low fluorescent glass gel plates (GE Healthcare) were soaked in 1% Contrad (Fisher Scientific), rinsed with ddH_2O, and polished with 200 proof ethanol prior to casting. Prior to ethanol polishing, plates previously used to cast bound gels were soaked in 1% HCL to hydrolyze residual bind-saline. The preparative gel sandwich back plates were treated with 4 ml of a bind solution containing 8 ml of 100% ethanol, 1.8 ml of ddH_2O, 200 µl of glacial acetic acid, and 12.5 µl of bind-saline (GE Healthcare). The bind solution was evenly spread over each back plate using Crewipes (Kimberly-Clark). After 2 h, fluorescent picking references (GE Healthcare) were placed on the back plates. Analytical and preparative gel sandwiches were assembled and loaded into a caster. A feed tube stem was inserted into the displacing solution reservoir, which was then filled with 90 ml of displacing solution (0.375 M TrisCl pH 8.8, 50% glycerol, and 0.002% bromophenol blue). A 12.5% acrylamide gel solution - containing 294 ml 40% monomer (GE Healthcare), 235 ml 1.5 M TrisCl (pH 8.8), 392 ml ddH_2O, 9.4 ml 10% sodium dodecyl sulfate (SDS), 376 µl *N, N, N', N,*-tetramethylethylethylenediamine (TEMED), and 9.6 ml ammonium persulfate (APS) - was prepared and poured into a funnel attached to the feed tube. The feed tube was removed, and the level of the gel solution was adjusted by adding additional displacing solution to the reservoir. The gels were allowed to polymerize for 2 h. After polymerization, excess polymer was trimmed from the edges of the plates, and the gel sandwiches were rinsed thoroughly with ddH_20. The gel

surfaces were covered with gel storage solution (0.375 M TrisCl, pH 8.8, 0.1% SDS), wrapped in plastic seal wrap, and then incubated overnight at room temperature before use.

Strip equilibration and second dimension. The IPG strips were thawed for 10 min at room temperature and then incubated twice in 20 ml of equilibration buffer (EB: 50 mM TrisCl, pH 8.8, 6 M urea, 30% glycerol, 2% SDS, 0.002% bromophenol blue) for 10 min at room temperature with shaking (80 rpm). During the first equilibration, the proteins were reduced by supplementing the EB with 0.5% DTT. During the second equilibration, the proteins were alkylated by supplementing the EB with 4.5 % iodoacetamide.

The gel sandwiches were rinsed with ddH_2O and inverted in a plate rack to drain excess liquid from the gel surfaces. Using forceps, the IPG strips were rinsed with electrophoresis running buffer (25 mM TrisCl, pH 8.3, 192 mM glycine, and 0.2% SDS), placed on the shelf of the gel sandwich (plastic backing against the back plate), and situated along the top of the second dimension gel using a plastic ruler. One milliliter of agarose sealing solution was added to the gel sandwiches. The proteins were separated (20W per gel at 20ºC until the dye fronts migrated off the gels) using an Ettan™ Dalt Twelve Large Format Vertical System (GE Healthcare) in the running buffer previously described. Analytical gels were imaged immediately. The top plates of the preparative gels were removed, and the gel bound bottom plates were placed in fixing solution (7.5% acetic acid, 10% methanol) in preparation for staining.

Staining of preparative gels. The preparative gels were incubated overnight in fixing solution and then stained with Deep Purple™ (GE Healthcare) according to the manufacturer's instructions. The gels were transferred directly from the fixing solution into a wash solution (35 mM sodium bicarbonate and 300 mM sodium carbonate) and incubated for 30 min with gentle shaking (25 rpm). After washing, the gels were incubated in 1 L ddH_2O for 5 min at 25 rpm. The

gels were then covered with 500 ml of a 200-fold dilution of Deep Purple™ stain and incubated in the dark for 1 h at 40 rpm. The gels were then incubated in 1 L of stabilization solution (7.5% acetic acid) for 1 h prior to imaging.

Scanning analytical gels. The gels were imaged with a Typhoon™ 9410 (GE Healthcare). Prior to scanning, the gel sandwiches were rinsed with ddH_2O and then dried completely. The scanner window was cleaned thoroughly with three rounds of 200 proof ethanol followed by ddH_2O. The gels were placed in the scanner oriented so that the top plate was up, the IEF strip was to the left, and the acidic portion of the gel was toward the user. The recommended emission filter / laser combinations were used for each dye.

A pre-scan at 1000 microns pixel intensity was conducted to optimize the PMT voltages for each fluor. The auto link mode was set to sensitivity, and the sensitivity was set to normal. The gels were scanned, and the PMT voltages were adjusted so that any increase in voltage resulted in the appearance of red saturation spots. Ten units were subtracted from this voltage, and it was used for scanning at 100 microns. The images were cropped using ImageQuant software, and the resulting 16-bit Tiff files were exported to Decyder™ Differential Analysis Software, Version 5.0 (GE Healthcare) for analysis.

Scanning preparative gels. While submerged in stabilization solution, cleaned glass top plates were lowed at an angle (to prevent trapping large bubbles) onto the top faces of the adhered preparative gels and then incubated for 5 min, allowing the top plates to stick to the gel surfaces. Prior to scanning, the gel sandwiches were rinsed with ddH_2O and then dried with Crewipes. Pre-scans were conducted as per analytical gels using the Green (532) laser and the 560LP emission filter. Images were acquired at optimized PMT voltages at 100 microns pixel

intensity and then exported to quantitative analysis software. The gel sandwiches were stored in stabilization solution at 4°C until spot picking.

Decyder™: analysis of analytical gels. The quantification of variations in protein levels between strains 6/85 and K5234 using DeCyder™ (GE Healthcare) was carried out, essentially, according to the user manual. For individual gels, the Differential In-gel Analysis (DIA) module was used to establish spot boundaries, convert pixel intensities to volumetric units, filter the images, normalize Cy™3 labeled and Cy™5 labeled samples against the Cy™2 internal standard, and calculate spot volume ratios. The Biological Variation Analysis (BVA) module was used for gel matching and the statistical analysis of variations.

DIA: sequential intra-gel analysis. Individually, the three images from each gel were opened in the DIA module. A value of 4,000 estimated spots was used. Spot detection and quantification was carried out with the triple detection function. A light filter using parameters established by GE Healthcare (slope, 1.1; area, 100; peak height, 100; and volume, 10,000) was applied.

BVA: simultaneous inter-gel analysis. Each image was assigned as an analysis image. The Cy™2 standard image with the most spots was assigned as the master image. For the purpose of statistical analysis, each image was assigned to one of three experimental groups: the two Cy™3 6/85 and the two Cy™5 6/85 images were assigned as controls, the two Cy™3 K5234 and the two Cy™5 K5234 images were assigned as variants, and the four Cy™2 standard images were assigned as standards. Extensive manual spot merging and land marking were conducted across the entire gel set. Spots were then matched. The matched images were intensively scrutinized, and incorrect matches were corrected manually. Statistical data was generated using a Student's T-test. The results were filtered by assigning all spots with a T-test

score below 0.01 and an average ratio above 1.5 or below -1.5 as proteins of interest. Each protein of interest was scrutinized again to ensure proper matching and spot boundary assignment.

Analysis of preparative gels. The preparative gel images were analyzed in the DIA module as per analytical gels using the single detection function. The gel images were incorporated into the previously established BVA file and assigned as pick gels. The location and size of the picking references were, if necessary, adjusted. Spots were merged where necessary, and the images were extensively landmarked against the master analytical images. The preparative images were then matched to the analytical gel set. Spots of interest that were correctly matched or could be manually matched to spots on the preparative image were assigned a pick status. The x and y coordinates of the confirmed spots were saved as a pick list.

Spot picking. Using an Ettan™ Spot Picker (GE Healthcare), the spots of interest were excised from the preparative gels according to the manufacturer's instructions. The top plates were removed from the gel sandwiches. The bound gels were appropriately oriented in the gel tray and covered with ddH_2O. The picker was primed 20 times with HPLC grade H_2O. Z-heights were determined for each gel. The gel plugs were transferred to low protein bind 96-well-plates (GE Healthcare) previously rinsed with ddH_2O. After picking, the water was removed from the wells, and the plugs were stored at 4°C until processing for MS.

Protein digestion. Protein digestion was carried out in the 96-well-plates. The gel plugs were incubated twice for 20 min in 100 µl of a wash solution containing 5mM ammonium bicarbonate and 50% acetonitrile (Applied Biosystems). The wash solution was removed, and 100 µl of 75% acetonitrile were added to each well. The samples were incubated for 20 min. The acetonitrile was removed, and the plugs were dried for 30 min in a speedvac. The 96-well-

plates containing the dehydrated plugs were handled with care to avoid sample loss due to static electricity. Seven microliters of fresh 20 µg/ml trypsin (Promega) in 20mM ammonium bicarbonate were added to the dehydrated plugs. The samples were incubated over night at 37°C. After digestion, 60 µl of 50% acetonitrile / 0.1% trifluoroacetic acid (TFA) was added to each well. The 96-well-plates were incubated for 20 min. The extracted peptides were transferred to low protein bind microfuge tubes (Fisher Scientific), and the extraction was repeated with 40 µl of the extraction solution. The second extracts were married to the first. The samples were dried down in a speedvac and stored at -20°C until de-salting.

De-salting. The dried down samples were solubilized in 1.5 µl of formic acid with vigorous vortexing. The volumes were brought up to 10 µl with 8.5 µl of 0.1% TFA. The samples were again vortexed and then centrifuged briefly. Samples were de-salted with µC18 ZipTips (Fisher Scientific) according to the manufacturer's instructions. The microtip columns were prepped by aspirating and dispensing 10 ul of wetting solution (50% acetonitrile in ddH_2O) twice and then equilibrated with ten rounds of 0.1% TFA. The samples were bound to the column by aspirating and despising the samples seven times. The bound peptides were then washed ten times with 10 µl of 1% TFA. The samples were eluted with 0.7 µl of elution solution (0.1% TFA and 70% acetonitrile) and spotted onto MS target plates. The spotted samples were allowed to partially dry, and then 0.3 µl of alpha matrix (Applied Biosystems) were added to each. The target plates were stored at room temperature protected from light until MS analysis.

Mass spectrometry. Mass spectrometry was conducted by the Macrochemical Facility at Emory University using an Applied Biosystems 4700 MALDI-TOF/TOF. The combined MS and MS/MS data was searched against the NCBInr database using the Mascot search engine. A protein score C.I. above 95% indicated identification or extensive homology.

CHAPTER 3

RESULTS

A total of over 1,000 spots were included in the 2DE analysis. This number may seem high for an organism containing only 742 genes, but it has been predicted that for prokaryotes 1.5 protein species exist for each gene (Simpson, 2003). Also, it must be kept in mind that a number of the spots were redundant, appearing in the overlapping region (ph 7) of the two types of IEF strips used, and that some spots were inevitably artifacts. Sixty-eight spots from the analytical gel sets showed fold changes above 1.5 or below -1.5 and had p-values below 0.01. Sixty of these spots were located as isolated spots on preparative gels and were subjected to MALDI-TOF/TOF for characterization. The digests from eight of these spots did not result in protein match scores indicative of identification, and four identifications were ambiguous. The remaining forty-eight digests had protein scores indicative of extensive homology or identification, forty of which, representing 29 different proteins, were identified as *M. gallisepticum* strain R_{low} protein species. These results are organized in Table 2 (p. 33). Fold changes are relative to K5234, positive numbers indicating an increased abundance in K5234 and negative numbers indicating a decreased abundance in K5234. Nine proteins appeared as multiple spots (multiple species). These included AtpD (ATP synthase beta chain), Lpd (dihydrolipoamide dehydrogenase), AcoA (pyruvate dehydrogenase), Mdh (lactate dehydrogenase), Smc-like protein (chromosome segregation ATPase), FusA (translation elongation factor G), MgpA-like protein (exopolyphosphatase related), HcaD (NADH oxidase), and a conserved hypothetical lipoprotein. All of the multiple forms of a given protein had the

same fold change direction. Twelve of the twenty-nine proteins increased in abundance, and 17 decreased. The highest positive fold change was 19.57 (one of the three AtpD species) and the lowest negative fold change was -9.13 (one of the two pyruvate dehydrogenase species). AtpA was the only protein of interest to appear on both 4-7NL and 7-11 gel sets.

Sixteen proteins of interest belong to COGs (Clusters of Orthologous Groups). The COGs represented include: [C] energy production and conversion, [D] cell division and chromosome partitioning, [F] nucleotide transport and metabolism, [G] carbohydrate transport and metabolism, [J] translation and ribosomal structure biogenesis, [K] transcription, [R] general prediction only, and [T] signal transduction. The most well represented COG is [C] energy production and conversion, with six proteins. Thirteen proteins of interest have no COG. Proteins with no COG represent 39% of the predicted *M. gallisepticum* proteome.

It should be mentioned that COGs are phylogenetic and not necessarily functional organizational tools. This discrepancy seems to be accentuated in mollicutes. Many of the activities typically associated with proteins encoded by mollicute genomes have not been detected in mollicutes. Some mollicute proteins have alternative or additional functions (bifunctionality) that are not reflected by their functional assignment. Additionally, some processes common to bacteria are mediated by proteins that have evolved independently in mollicutes and are thus phylogenetically unrelated to proteins that mediate similar processes in other bacteria. Functional classification is further complicated by significant protein functional variability within class *Mollicute* (Pollock, 2002).

Three of the unclassified proteins are considered virulence factors. These include GapA (*M. gallisepticum* adherence protein A), CrmA (cytadherence related molecule A), and VlhA.3.09 (pMGA family protein) – all three of which had increased levels in the virulent field

strain. Three proteins of interest are conserved hypothetical proteins, and three are unique hypothetical proteins. Generally, proteins associated with virulence increased in abundance in the virulent K5234, while metabolic proteins decreased in abundance in K5234.

Table 2. Differential and MS data. Fold changes are relative to K5234 (the virulent field isolate). Positive numbers indicate increased abundance in K5234, and negative numbers indicate decreased abundance in K5234. (-) indicates multiple forms of the same protein, except in the case of AtpA, which appeared in both experimental sets (Tatusov et al., 2001; Barre et al., 2004).

Protein	Description	Locus	Accession #	**Fold Δ**	p-value	MS C.I.%
[C] Energy production and conversion						
AtpD	ATP synthase beta chain	MGA_491	31541707	**19.57**	$7.6x10^{-5}$	98.3
-	-	-	-	**11.19**	$1.5x10^{-5}$	100
-	-	-	-	**6.02**	$2.2x10^{-6}$	100
AtpA (4-7)	ATP synthase alpha chain	MGA_488	31541706	**3.76**	$7.5x10^{-6}$	100
- (7-11)	-	-	-	**3.09**	$1.9x10^{-4}$	100
Lpd	Dihydrolipoamide Dehydrogenase	MGA_161	31541532	**2.61**	$6.3x10^{-6}$	100
-	-	-	-	**2.60**	$1.5x10^{-5}$	100
AcoA	Pyruvate dehydrogenase	MGA_165	31541535	**-9.13**	$1.6x10^{-6}$	100
-	-	-	-	**-4.13**	$5.0x10^{-3}$	99.7
Mdh	L-lactate Dehydrogenase	MGA_746	31541121	**-1.85**	$7.3x10^{-6}$	100
-	-	-	-	**-1.71**	$3.0x10^{-3}$	100
AceF	Dihydrolipoamide acetyltransferase	MGA_162	31541533	**-1.71**	$3.2x10^{-8}$	100
[D] Cell division and chromosome partitioning						
Smc-like	Chromosome segregation ATPase	MGA_917	31541218	**1.98**	$4.9x10^{-7}$	100
-	-	-	-	**1.86**	$2.6x10^{-5}$	100
FtsZ	Cell division protein	MGA_27	31541447	**-1.60**	$3.6x10^{-6}$	100
[F] Nucleotide transport and metabolism						
NrdF	Ribonucleotide reductase beta subunit	MGA_698	31541093	**-2.84**	$5.0x10^{-5}$	100
NrdA	Ribonucleotide reductase alpha subunit	MGA_695	31541091	**-1.97**	$1.3x10^{-5}$	100
[G] Carbohydrate transport and metabolism						

Eno	Enolase	MGA_209	31541555	**-2.63**	$1.2x10^{-3}$	100
[J] Translation, ribosomal structure biogenesis						
FusA	Translation elongation factor G	MGA_260	31541582	**1.71**	$8.3x00^{-5}$	100
-	-	-	-	**1.54**	$1.6x10^{-4}$	100
[K] Transcription						
NusA	N-utilization substance protein A homolog	MGA_818	31541161	**1.57**	$1.6x10^{-4}$	100
[R] General prediction only						
MgpA-like	Exopolyphosphatase related	MGA_683	31541085	**-1.97**	$7.3x10^{-8}$	100
-	-	-	-	**-1.65**	$6.8x10^{-6}$	99.8
Predicted GTPase		MGA_500	31541712	**-1.56**	$3.4x10^{-7}$	100
[T] Signal transduction						
PTC1	Protein serine/threonine phosphatase	MGA_461	31541689	**-1.89**	$5.5x10^{-6}$	100
Unclassified						
CrmA	Cytadherence related molecule A	MGA_939	31541229	**3.88**	$7.1x10^{-8}$	100
GapA	*M. gallisepticum* adherence protein A	MGA_934	31541228	**2.17**	$3.9x10^{-3}$	100
TrxB	Thioredoxin reductase	MGA_1221	31541379	**1.91**	$4.6x10^{-7}$	100
Gmk	Guanylate kinase	MGA_462	31541690	**-1.61**	$7.2x10^{-3}$	100
HcaD	NADH oxidase	MGA_167	31541536	**-1.60**	$1.8x10^{-4}$	99.4
-	-		-	**-1.60**	$5.8x10^{-6}$	100
GryB	DNA gyrase (topoisomerase) B subunit	MGA_616	31541775	**-1.56**	$1.6x10^{-4}$	100
VlhA.3.09	pMGA family protein; similar to pMGA1.4.1.3	MGA_395	31541647	**-3.70**	$9.9x10^{-5}$	100
Conserved hypothetical						
Conserved hypothetical, lipoprotein		MGA_267	31541586	**1.91**	$4.4x10^{-7}$	100
-		-	-	**1.73**	$5.8x10^{-7}$	100
Conserved hypothetical, lipoprotein		MGA_674	31541080	**-1.63**	$2.2x10^{-3}$	100
Conserved hypothetical (Hlp2)		MGA_1203	31541370	**-1.59**	$2.2x10^{-5}$	98.3

Unique hypothetical					
Unique hypothetical (COG)	MGA_480	31541701	**2.50**	$1.2x10^{-3}$	100
Unique hypothetical	MGA_573	31541754	**1.82**	$1.6x10^{-6}$	100
Unique hypothetical	MGA_1071	31541293	**-2.10**	$7.2x10^{-6}$	99.1

CHAPTER 4

DISCUSSION

Phase / antigenic variation and VlhA

The ability of bacterial populations to persist or proliferate in constantly changing environments is often based on their ability to vary phenotypes (phenotypic plasticity), either in response to environmental cues or by random mutations. Phenotypic variation via environmental sensing is typically achieved through a mechanism whereby an organism "samples" its environment and adjusts its phenotype accordingly via a sensor/response regulator system (Rottom, 2003). For example, *Pseudomonas aeruginosa* is thought to switch between a virulent, free-living state and a less virulent but more persistent biofilm state in response to available nutrient and energy sources (O'Toole, 2004).

An alternative means of phenotypic variation employed by many bacteria, especially those with limited genetic capacities and few regulatory proteins, is phase or antigenic variation. Generally, both phase and antigenic variation refer to the ability of an organism to alternate between phenotypes in a "heritable and reversible manner" (van der Woude and Baumler, 2004). Within this broad definition, specific definitions of phase and antigenic variation continue to evolve as more relevant data is produced. The most contemporary use of 'phase variation' refers to the oscillation of a gene between all 'on' and all 'off' states. In contrast, 'antigenic variation' refers to the oscillation between different antigenic forms. Sometimes this involves gene families, which can act as archives of epitopes, expressing only one epitope at a time (van der Woude, 2006). Simplistically, with the former, the protein is either present or absent, and with the latter, the protein or structure is typically present but in different forms.

Both phase and antigenic variation generate heterogeneous populations of clonal variants by high frequency random mutations which occur as replication errors. The phase of the parent cell is passed along to the daughter cell, which can then generate revertants. While the mutations are thought to be random and thus non-responsive to the environment, the frequencies of the mutations can be modulated, and current research indicates that phase variation may be integrated into regulatory networks that *are* environmentally responsive. The functions of structures that undergo phase/antigenic variation vary, but most are antigenic surface structures (i.e. surface appendages and lipoproteins) or enzymes involved with modifying these surface structures (van der Woude, 2006). The biological significance of phase/antigenic variation is most commonly thought to endow pathogens with a means of evading host immune responses, which target individual cells expressing dominate antigenic forms while allowing subpopulations of antigenic variants to escape and proliferate, causing chronic infections (Frank and Barbour, 2006; Lipsitch and O' Hagan, 2007). Recent studies indicate that phase/antigenic variation is not limited to host/pathogen interactions but can also be the bases of numerous adaptive processes, including niche exploitation (van der Woude, 2006). In the current study, three of the virulence factors (VlhA, GapA, and CrmA) that varied in abundance undergo phase and/or antigenic variation.

VlhA (previously designated pMGA), a family of surface lipoproteins, is the immunodominant antigen of *M. gallisepticum* recognized by chicken antibodies. VlhAs are hemmagluttinins and have been shown to undergo both phase and antigenic variation *in vitro* and *in vivo* (Bradbury, 2005; Markham et al., 1992). *Mycoplasma gallisepticum* strains analyzed thus far have VlhA families consisting of from 32 to 51 genes, attesting to its importance to *M. gallisepticum* survival (Basseggio et al., 1996). The prototype stain R_{low} has 49 *vlhA* genes

(Szczepanek et al., 2010). Early studies interpreted the presence of different vlhA transcripts within a single population as multiple *vlhA* transcription at the cellular level (Glew et al., 1995); however, current studies indicate that the expression of different VlhA paralogues within a population results from small subpopulations that happen to express different family members, and that at the cellular level only one family member is transcribed at any given time (Liu et al., 2000).

In vitro expression of VlhA in isogenic lineages oscillates in response to the presence or absence of VlhA directed antibodies. Markham et al. demonstrated that when grown in the presence of an antibody directed at VlhA1.1 (the designation of the predominate VlhA protein expressed in culture without antibody pressure), *M. gallisepticum* S6 ceased expressing VlhA1.1 and immediately began expressing a secondary, antigenically distinct family member, designated VlhA1.9. When the VlhA1.9^{+} progenitor cells were transferred back into media lacking the antibody, the population ceased expressing VlhA1.9 and reverted to the phenotype of the founder cells (Markham et al., 1998). Glew et al. observed a slightly different scenario *in vivo*. Chickens were inoculated with strain S6, and six days post infection the majority of the recovered cells ceased to express any VlhA family member. Only after prolonged incubation did a population arise that expressed a paralogue different from that of the inoculant. Thus, a phase variant dominated the acute stage of infection, while an antigenic variant dominated the chronic stage of infection. Interestingly, unlike the *in vitro* study mentioned above, the *in vivo* variant population arose and proliferated prior to the appearance of detectable antibodies. The authors hypothesized that there might have been some growth advantage that selected for the VlhA phase variant (Glew et al., 2000). The nature of these phenotypic switches was shown to be transcriptional,

involving high frequency alterations in the number of short tandem GAA repeats in the intergenic regions of *vlhA* family members (Glew et al., 1998; Liu et al., 1998; Liu et al., 2000).

A recent analysis of global transcript variations between *M. gallisepticum* cells grown in broth versus cells grown in association with eukaryotic cells showed that one VlhA paralogue was up-regulated 2.41 fold in cells grown in association with eukaryotic cells (Cecchini et al., 2007). Interestingly, by setting the incubation time below that of a generation time, the study was designed in way as to negate the influence of phase/antigenic variation and only include variations resulting from transcriptional regulation in response to environmental cues. A genomic comparison of the virulent R_{low} strain with the attenuated F strain revealed that the *vlhA* locus was the most highly variable genomic region between the two strains, with F strain containing 28 fewer family members than R_{low} (Szczepanek et al., 2010). This data further supports the involvement of VlhA in the adaptation of *M. gallisepticum* to its environment.

In the current study, the attenuated vaccine strain (6/85) expressed 3.7 fold more VlhA.3.09 than did the virulent 6/85-like field isolate (K5234); no other VlhA appeared in the data set. As previously mentioned, individual *M. gallisepticum* cells express only one or no VlhA family member at any given time , and other than being all ‘on’ or all ‘off’ (Liu et al., 2000), there are no reports of *M. gallisepticum* cells varying the expression of any one family member. Likewise, there are no reports which indicate that, at the cellular level, one strain of *M. gallisepticum* produces significantly more or less VlhA than another strain. So while it cannot be dismissed that individual 6/85 cells may have simply contained more VlhA.3.09 than K5234 cells, it is more likely that the experimental variations occurred at the population level: more cells in the 6/85 population expressed VlhA.3.09 than did cells in the K5234 populations. With this in mind, one possible scenario to account for the experimental variation is that VlhA.3.09

could have been the predominant (that member expressed in the absence of antibodies) family member expressed by 6/85 populations and only a secondary family member expressed by K5234 populations. In this case, K5234 may have expressed its predominant VlhA in higher levels than the same family member was expressed in 6/85, but the variation was not detected by the analysis. Alternatively, VlhA.3.09 could have been the predominant VlhA for both strains, with K5234 populations generating a higher number of phase variants which expressed no VlhA family member. If the two strains do in fact express different predominate VlhAs during the initial stage of infection, the epitope of the VlhA expressed by K5234 could elicit a stronger antibody response than VlhA.3.09, contributing to the enhanced infectivity of K5234. The predominant VlhA of K5234 may also have enhanced functionality when compared to VlhA3.09. VlhAs have been shown to mediate the attachment of *M. gallisepticum* to chicken erythrocytes (Markham et al., 1992), and, recently, it was discovered that *M. gallisepticum* is capable of invading erythrocytes and is commonly found in the bloodstream of infected chickens (Vogl et al., 2008). It follows that enhanced VlhA functionality could aid both the dissemination of the pathogen within the host and the evasion of the host's immune response. Regarding the latter scenario, in which K5234 was predisposed to generate phase variants at a higher frequency than 6/85, it has been demonstrated that VlhA phase variants can dominate the acute stages of infection (Glew et al., 2000). VlhA phase variants could hide from the host's immune response by not expressing any VlhA, replacing the function of VlhA with an alternative adhesin. Alternatively, phase variants may be more suitable for colonization during early infection. VlhAs are known to self-interact (Markham et al., 98), causing the clumping of cells which may actually detract from the organism's ability to spread along a surface. If, indeed, the 3.7-fold decrease in VlhA.3.09 reflects a higher abundance of phase variants in the K5234 experimental

populations, it is also possible that the increased frequency of variants resulted from an unknown regulatory activity rather than the predisposition of the organism. In lieu of the experimental findings and previous research involving VlhA, variations in VlhA expression likely play a role in the enhanced virulence and persistence of K5234 as compared that of 6/85.

Adhesins

Cytadherence is considered a prerequisite for the pathogenesis of many mollicutes, and adhesins are often considered the primary virulence factors of these organisms (Rottom, 03). After being inhaled, mollicute respiratory pathogens often adhere to the epithelial cells of the host's respiratory tract (Bradbury, 05). Strong adherence prevents the immediate clearing of the organism by the host's immune system, allowing the initiation of other colonization mechanisms, such as motility, cell invasion, and biofilm formation. The best studied mollicute adherence system is that of *M. pneumoniae*, which localizes adhesins at one end of the cell in what is called a terminal tip organelle (or attachment organelle) (Rottom, 03). While the attachment of *M. gallisepticum* is not as well elucidated as that of *M. pneumoniae*, *M. gallisepticum* does possess a terminal tip organelle and has several adhesins which are homologous to those of *M. pneumoniae*, two of which appeared in this study (Fig. 6, p. 58).

GapA, which increased 2.27-fold in K5234, has been implicated in *M. gallisepticum* cytadherence and is, like VlhA, phase variable (Papazisi et al., 2003). The putative function of GapA was determined by searching the genome of *M. gallisepticum* for homologues to the well-studied adhesions of *M. pneumoniae* and *M. genitalia*, which belong to the same phylogenic cluster as *M. gallisepticum*. A gene was located that shared 45% homology to the *M. pneumonia* P1 adhesin and 46% homology to the *M. genitalium* MgPa adhesin, both of which are the

primary adhesin in there respected organism (Goh et al., 1998). This putative adhesin gene was located at the beginning of a multi-gene operon and was designated *gapA* (*M. gallisepticum* adherence protein A). In tracheal ring attachment inhibition assays, labeling *M. gallisepticum* cells with a GapA antagonist resulted in reduced attachment by 64% (Goh et al., 1998). Several other assays, both *in vitro* and *in vivo*, have demonstrated that GapA is essential to *M. gallisepticum* cytadherence (Papazise et al., 2000; Papazise, 2002 et al., Mudahi-Orenstein et al., 2003).

In order for *M. gallisepticum* to attach to host cells and cause infection, *gapA* expression must co-occur with the expression of *crmA* (Papazise et al., 2002). CrmA expression increased 3.88 fold in K5234. The function of *crmA* was determined, in part, by comparing the protein expression profile of the avirulent, attenuated *M. gallisepticum* R_{high} strain with its virulent progenitor, strain R_{low}. Papazise et al. identified three proteins present in R_{low} that were absent in R_{high}. One of the absent proteins was GapA. The gene of another absent protein was located immediately downstream from *gapA* and shared significant sequence homology to genes encoding attachment accessory molecules in *M. pneumoniae* and *M. genitalium*. This putative cytadherence gene was designated *crmA* (cytadherence related molecule) (Papazisi et al., 2000). In cell culture attachment assays, attachment of the avirulent R_{high} strain was 75% less than that of the virulent R_{low} strain. Complimenting R_{high} with wild type *gapA* or *crmA* did not restore wild type levels of attachment; however, complementing R_{high} with the entire R_{low} *gapA* operon, containing both *gapA* and *crmA*, did result in attachment and virulence phenotypes *in vitro* and *in vivo* (Papazisi et al., 2002). Comparative sequence analysis of *gapA* and *crmA* indicates that they might interact with each other in the cytoplasm, implying that not only co-expression but also coordinated action between the two proteins may be necessary for attachment (Papazise et al.,

2003). This is consistent with the functions of homologues in *M. pneumoniae* (Krause, 2001). Transposon mutagenesis studies conducted by Orenstein and co-workers confirmed that GapA and CrmA are essential to the cytadherence and virulence of R_{low}. Of the 3,500 mutans screened, only 5 had attachment and avirulent phenotypes. Two of these contained transposons in *gapA* and one contained a transposon in *crmA*. (Mudahi-Orenstein et al., 2003).

GapA/CrmA expression is phase variable. Phase variants arise as a consequence of a reversible nonsense mutation at the beginning of the *gapA* gene and not as a consequence of the deletion or addition of intergenic trinucleotide repeats, as is the case for VlhA. The mechanism by which the reversible nonsense mutation is achieved is unknown; it cannot be reconciled with slipped-strand mispairing, the mechanism (not well understood itself) used to explain the DNA replication error that promotes trinucleotide repeat mediated phase variation (Rosengarten et al., 2000; Winner et al., 2003).

Together, this data demonstrates that GapA and CrmA are essential to the cytadherence and virulence of *M. gallisepticum* R_{low}. Cytadherence not only enables bacteria to avoid host clearance, it is also a prerequisite for other physiological activities associated with mollicute pathogenesis, like cellular invasion and motility (Much et al., 2002; Nakane et al., 2009). Increased levels of GapA and CrmA in the virulent field strain (K5234) may have contributed to its increased persistence, colonization, and virulence.

Energy metabolism and housekeeping enzymes

Many of the proteins in the data set provide basic metabolic functions. The role these "housekeeping enzymes" might potentially play in pathogenicity is typically overlooked. But "housekeeping genes may confer virulence" (Pollack, 2002). Hudson et al. note:

> Traditionally, the Lpd protein [dihydrolipoamide dehydrogenase of *M. gallisepticum*] would be considered a metabolic factor, and therefore, its role in pathogenicity might never be investigated…The definition of what constitutes a virulence-associated determinant is not limited to toxins and cytadhesins, but also includes proteases, regulatory proteins, stress response proteins, transport proteins, and proteins involved in metabolism. A virulence-associated determinant is therefore defined as any factor that confers a selective advantage on the pathogen, allowing it to colonize the host, persist, propagate, and cause disease (Hudson et al., 2006).

The relevance of housekeeping enzymes as virulence factors has been heightened by the discovery that many housekeeping enzymes, including all five enzymes of the triose portion of glycolysis, can localize on the cell surface of prokaryotes, with several capable of mediating the attachment to host cell fibronectin and plasminogen (Pancholi and Chhatwal, 2003). While it is difficult to reconcile most of the variations in abundance of metabolic enzymes in the current study with *known* mechanisms of *M. gallisepticum* virulence, these proteins may have contributed to the increased persistence and virulence of K5234, and thus they warrant discussion.

The primary locus of fermentative mollicute metabolism is pyruvate. Mollicutes are capable metabolizing pyruvate to lactate, acetyl-CoA, or oxaloacetate (Fig. 7, p. 59) (Hudson et al., 06; Razin et al., 98). With the exception of one of the three components of the pyruvate dehydrogenase complex (PDHC), the enzymes responsible for the conversions of pyruvate to lactate and acetyl-CoA decreased in abundance in the virulent field strain (K5234) as compared with the attenuated vaccine strain (6/85). These enzymes included lactate dehydrogenase (Mdh) and two of the three enzymes of the PDHC, pyruvate dehydrogenase (AcoA) and dihydrolipoamide acetyltransferase (AceF). The third PDHC enzyme, dihydrolipoamide dehydrogenase (Lpd), showed increased levels in K5234.

As mentioned in the introduction, fermentative mollicutes possess complete glycolytic pathways but lack TCA cycles, cytochromes, and quinones and are thus incapable of generating ATP by oxidative phosphorylation. Most of their ATP is thought to be produced by substrate-level phosphorylation during glycolysis (Pollock, 02). Glycolysis relies on the electron accepting role of NAD^+, which is reduced to NADH and must be regenerated in order for glycolysis to continue. In mollicutes, the major pathway for regenerating NAD^+ is the reduction of pyruvate (the end product of glycolysis) to lactate, with the concomitant re-oxidation of NADH to NAD^+ (Equation1). This conversion is catalyzed by lactate dehydrogenase (the Mdh protein in *M. gallisepticum*), which decreased -1.85, -1.71, and -1.68 fold in the current study (Figure 3). The malate dehydrogenase activity observed in some mollicutes is also attributed to lactate dehydrogenase and will be discussed later (Pollock et al., 97).

Equation 1: $\text{Pyruvate} + \text{NADH} \rightarrow \text{Lactate} + NAD^+$

It has been shown in several fermentative mollicutes that lactate dehydrogenase is de-activated by reduced levels of fructose1,6-bisphosphate (the final metabolite of the hexose portion of glycolysis) and it is hypothesized that this feed forward inhibition shunts pyruvate toward acetyl-CoA and/or oxaloacetate and away from lactate and the re-oxidation of NADH to NAD^+. The assumption is that under growth limiting conditions, where glycolytic activity is being reduced due to limited substrate, cells are less reliant on the regeneration of NAD^+ and may benefit from having fewer resources invested in the lactate pathway (Pollock, 02). This also may increase the viability of a dense cell populations by decreasing the amount of lactate secreted into the environment, as lactate production is accompanied by the acidification of the

cellular milieu, which has been shown to inhibit cell growth at high cell densities (Pollock et al., 97).

In addition to lactate, mollicutes can also convert pyruvate to acetyl-CoA by the PDHC, a ternary complex composed of dihydrolipoamide dehydrogenase, dihydrolipoamide acetyltransferase, and pyruvate dehydrogenase (Equation 2). Dihydrolipoamide acetyltransferase (-1.71/-1.64) and pyruvate dehydrogenase (-9.13/-4.13) showed reduced levels in K5234, while dihydrolipoamide dehydrogenase (2.61/2.60) showed increased levels. Additional ATP can be generated by substrate-level phosphorylation with the conversion of acetyl-CoA to acetate (Equation 3) (Halbedel et al., 2007; Madigan et al., 2009). However, the ATP generated by this pathway is not thought to contribute significantly to the total ATP pool. Acetate is an important precursor for fatty acid synthesis in most mollicutes (Pollock et al., 97).

Equation 2: $\text{Pyruvate} + \text{CoA} + \text{NAD}^+ \rightarrow \text{Acetyl-CoA} + \text{CO}_2 + \text{NADH}$

Equation 3: $\text{Acetyl-CoA} + \text{Pi} \rightarrow \text{Acetyl-phosphate}$

$\text{Acetyl-phosphate} + \text{ADP} \rightarrow \text{Acetate} + \text{ATP}$

Of the enzymes involved in pyruvate metabolism that are represented in the dataset, dihydrolipoamide dehydrogenase is the only one that has been linked to virulence in *M. gallisepticum* (Hudson et al, 06). The role of dihydrolipoamide dehydrogenase in the PDHC is to re-set the redox state of the complex toward the end of the conversion of pyruvate to acetyl-CoA so that the PDHC can continue to function (White, 2000). Hudson et al. identified dihydrolipoamide dehydrogenase as a potential virulence determinant using signature sequence mutagenesis (SSM), an *in vivo* technique which involves inoculating a single animal with a pool

of tagged transposon mutants. If a mutant is unrecoverable, then it is hypothesized to contain a transposon in a gene essential for *in vivo* survival, and thus the gene product is identified as a potential "virulence-associated determinant." Of the 27 mutants inoculated into chickens, the only one that was not recovered from the tissue tested contained a transposon in the dihydrolipoamide dehydrogenase gene. When compared to the wild type strain (the virulent R_{low}), protein homogenates from the dihydrolipoamide dehydrogenase mutant showed decreased PDHC activity *in vitro*. The mutant was also attenuated *in vivo*. The authors concluded that the lack of functional dihydrolipoamide dehydrogenase rendered the PDHC inoperative after one reaction, decreasing the amount of ATP that could potentially be produced by the conversion of acetyl-CoA to acetate, causing a growth defect which was masked *in vitro* but manifest *in vivo* (Hudson et al., 06). In a follow up study, the authors evaluated the SSM Lpd mutant as a vaccine candidate. Under the experimental condition employed, the Lpd mutant outperformed the vaccine strains ts-11 and F-strain (Gates et al., 2008). Recently, in *Mycobacterium tuberculosis*, dihydrolipoamide dehydrogenase was shown to be a component of two enzyme complexes other that the PDHC. Both enzyme complexes are colonization factors, one provides protection from host born reactive nitrogen intermediates and the other prevents the accumulation toxic intermediates of amino acid metabolism (Venugopal et al., 2011). These activities have not been investigated in *M. gallisepticum*, but they may exist and may have contributed to the attenuation of the Lpd mutant discussed above. Lastly, in a study which compared the transcriptomes of *M. gallisepticum* cells grown in broth versus cells grown in association with eukaryotic cells, dihydrolipoamide dehydrogenase was reported to be downregulated 2.28 fold in attached cells (Cecchini et al., 07). Interestingly, lactate dehydrogenase (-3.50) and dihydrolipoamide acetyltransferase (-2.22) were also shown to be downregulated. As previously mentioned, these

two enzymes showed a decreased abundance in K5234. The downregulation of PDHC enzymes and lactate dehydrogenase in the transcriptome study suggests a decreased dependence on the conversion of pyruvate to lactate and acetyl-CoA in what is thought to be a more persistent lifestyle.

In addition to lactate and acetyl-Co, the other major product of pyruvate metabolism in mollicutes is oxaloacetate (OAA) (Equation 4). Oxaloacetate can be used as a substrate for amino acid biosynthesis, or it can be converted to malate by the activity of lactate dehydrogenase (Equation 5). As with the production of lactate, malate production is accompanied by the regeneration of NAD^+. It is thought that the malate pathway may provide organisms with a means of producing NAD^+ without the deleterious effects of the acid production associated with the lactate pathway. In mollicutes, low malate dehydrogenase activity has been associated with a decreased dependence on NAD^+ regeneration and an increased flow of oxaloacetate to amino acid biosynthesis (Pollock et al., 97; Pollock, 02).

Equation 4: $\text{Pyruvate} + \text{ATP} + CO_2 \rightarrow \text{OAA} + \text{ADP} + \text{Pi}$

Equation 5: $\text{OAA} + \text{NADH} \rightarrow \text{Malate} + NAD^+$

The evidence that some mollicutes funnel pyruvate away from lactate and malate under growth limiting conditions, and that *M. gallisepticum* downregulates lactate dehydrogenase and two of the three enzymes of the PDHC when grown in contact with eukaryotic cells suggests a possible correlation between the increased persistence of K5234 in the field trials and the decreased levels of lactate dehydrogenase and the PDHC enzymes observed in the current study. One possible explanation is that K5234 is a more effective parasite, in that it may be able to

acquire more metabolic precursors from its host and is thus less dependent on energy metabolism producing the necessary ATP needed for macromolecular subunit biosynthesis. Another possible scenario is that the decreases reflect a metabolic state that is more conducive to long term persistence in a substrate limiting environment, and that K5234 achieves this state by either investing fewer resources in pyruvate metabolism in general or by funneling pyruvate away from lactate and acetate at the pyruvate locus, or both. If this were to be the case, then either K5234 is simply genetically predisposed toward this state, or it is more effective at regulating metabolic enzymes than is 6/85. In either case, the variation would have to have been masked in the nutrient rich, *in vitro* growth media, where the two strains had similar growth curves, but become apparent in the more competitive and limiting *in vivo* environment. If the variations involved variable regulation, the obvious question is why this shift toward stationary phase growth occurred *in vitro* during mid-exponential phase in K5234, and also why it occurred in K5234 and not 6/85. It has been reported that variations in the expression of metabolic enzymes observed during transitional phase cells of some bacteria actually begin in mid-exponential phase growth (Cohen et al., 2006). Decreases in the abundance of FtsZ (-1.60), NrdA (-1.97), and NrdF (-2.84, -1.95) in K5234 could also indicate preparation for slower growth. FtsZ (filamentous temperature sensitive - Z) is a tubulin-like protein that initiates cell division by polymerizing into a ring around the center of a growing cell (Madigan, et al., 2009). The decrease in abundance of FtsZ could simply reflect a decrease dependence on FtsZ specifically for cell division, as the protein was recently found to be nonessential to cell division in *M gallisepticum's* close relative *M. genitalium* (Lluch-Senar and Piol, 2010). Two subunits of ribonucleotide reductase (NrdA and NrdF) showed a decreased abundance in K5234. Ribonucleotide reductase reduces ribonucleotides to deoxyribonucleotides in preparation for chromosomal replication (Madigan et

al., 2009). It is possible that by an unknown regulatory system K5234 begins preparing for stationary phase growth before 6/85 does, and that this is not reflected in the growth curves of the two strains, though it may manifest with prolonged, late stationary phase growth, which was not included in the experimental growth curves. Perhaps the regulation of metabolism in K5234 is slightly different and more sensitive than that of 6/88. Also, in a substrate limiting environment, K5234 may be less dependent upon fatty acid biosynthesis and benefit from having fewer resources invested in the acetate pathway.

While no significant change in the abundance of the enzymes needed to convert oxaloacetate to amino acids was detected by in this study, it is possible that K5234, when compared with 6/85, funnels less pyruvate toward lactate and acetyl-CoA and more pyruvate toward amino acids and protein biosynthesis, perhaps toward the synthesis of structural proteins that are directly associated with persistence and virulence – like GapA, CrmA, and VlhA. It is of interest that while lactate dehydrogenase and the PDHC enzymes were down-regulated in the Cecchini et al. study, numerous ribosomal proteins were up-regulated, indicating a generalized increase in translation (Cecchini et al., 2007). In the current study, FusA, a translation elongation factor, increased in abundance in K5234. This, likewise, could indicate an increase in translation.

Other proteins of interest

The most conspicuous aspect of the results is the high fold change of AtpA (ATP synthase alpha chain) and AtpD (ATP synthase beta chain); the former increased 3.76/3.09 and the latter increased 19.57/11.19/6.02 in K5234. As previously mentioned, mollicutes are incapable of generating ATP at the expense of the proton motive force, a process catalyzed by ATPase. Mollicutes possess ATPase, but their ATPase acts only in reverse, using energy from

ATP hydrolysis to establish ion gradients by pumping hydrogen or sodium ions out of the cell membrane. In addition to their role in ATP synthesis, ion motive forces are also used to drive cellular activities like membrane transport and motility (Pyrowolakis et al., 1998; White, 2000). However, it has been demonstrated that the gliding motility exhibited by mollicutes is driven by the direct hydrolysis of ATP (like Type IV pila mediated motility), as opposed to being driven by ion motive forces (like flagella mediated motility) (Charon, 2005; Jaffe et al., 2004).

The ATPase of *M. gallisepticum* has the same eight subunits that compose the typical bacterial F-type ATPase, with AtpA and AtpD composing the catalytic portion of the complex (Rasmussen et al., 1992). However, the AtpA and AtpD that increased in abundance in this study seem to be additional variants, possessing a PS00107 protein kinase motif, and their chromosomal location is different than that of the other eight subunits (Gutman et al., 2005; Papazisi et al., 2003). It is unclear, but perhaps *M. gallisepticum* has variable ATPases, some containing conventional AtpA and AtpD subunits and others containing variant subunits. Due to the high fold change of these two proteins and the importance of ATPases to cellular physiology, further investigation into the function of these ATPase subunit variants is warranted.

Thioredoxin reductase (TrxB) increased 1.91 fold in K5234. Along with thioredoxin, thioredoxin reductase is a component of the $NADP^+$ / thioredoxin system (NTS). The NTS is involved in numerous processes in eukaryotes, but little is known about its function in prokaryotes. “Although the magnitude of the role of [the] thioredoxin-reductase system…in mollicute metabolism is presently not certain, we imagine that it is significant,” writes one researcher (Pollock, 2002). It has been reported that the mollicute NTS is capable of protecting cells from the deleterious effects of reactive oxygen species (ROS) by transferring electrons from NADPH (the origin of the NADPH is not known) to proteins and low molecular weight

molecules (Fig. 8, p. 60), thereby maintaining them in their functional reduced forms and protecting them from deleterious oxidation by host-born and native ROS - such as superoxide, hydroxyl radicals, and H_2O_2, and organic peroxides (Ben-Menachem et al., 1997; Koharyova and Kollarova, 2008; Pollack, 2002). Mollicute infection sites contain an abundance of ROS, mainly H_2O_2. Hydrogen peroxide is considered a virulence factor of mycoplasmas and is also produced by host phagocytes (Madigan 09 et al.; Jenkins et al., 2008). The NTS of other bacteria provides protection from nitric oxide and reactive nitrogen species, and the thioredoxin reductase of mycobacteria has been discussed as a potential drug target (Jaeger et al., 2006; Qu et al., 2009). As mollicutes lack catalase and peroxidase activities (Pollock, 2002), NTS may be their primary defense mechanism against ROS, and elevated levels of TrxB could enhance both colonization and virulence.

Equation 6: $$\text{Trx-S}_2 + \text{NADPH} + \text{H}^+ \rightarrow \text{Trx-(SH)}_2 + \text{NADP}^+$$
$$\downarrow$$
$$\text{Protein-S}_2 + \text{Trx-(SH)}_2 \rightarrow \text{protein-(SH)}_2 + \text{Trx-S}_2$$

The presence of guanylate kinase (Gmk) in the data set is of interest because it is one of the very few *M. gallisepticum* proteins that possesses motifs indicative of regulatory proteins. Thus far, no conventional regulatory proteins have been described in *M. gallisepticum* (Papazisi et al., 2003).

Hypothetical proteins

Six conserved or hypothetical proteins varied in abundance between the two strains. Two of these proteins have been renamed since the initial sequencing of strain R_{low} and the

completion of the current study. MGA0674, which decreased 1.63-fold, is now named MslA, for *Mycoplasma*-specific lipoprotein A, and MGA1203, which decreased 1.59-fold, is now named Hlp2, for high molecular weight (HMW) 3-like protein (May et al., 2006; Szczepanek et al., 2010b). MslA has appeared in two global transcript studies. In a transcriptomic comparison of strain R_{low} cells grown in broth versus cells grown in association with eukaryotic cells, MslA was downregulated 2.5-fold, the same fold-change direction as in this study (Cecchini et al., 2007). However, MslA transcripts were 6-fold more abundant in the virulent R_{low} strain than the attenuated F strain. Szczepanek and co-workers reported that MslA was immunogenic, and that mutants with transposons in *mslA* had reduced recovery and attenuated virulence *in vivo*. The role MslA plays in *M. gallisepticum* physiology and pathogenesis is yet to be determined (Szczepanek et al., 2010b). Hlp2, which also decreased in abundance in K5234, is classified as a cytadherence-related protein based on homology to the *M. pneumonia* protein HMW2 (May et al., 2006). HMW2 is a major component of the *M. pneumonia's* terminal tip structure and is involved in the localization of numerous proteins that mediate not only attachment and gliding motility but also cell division (Bose et al., 2009; Hasselbring et al., 2006). Hlp2 is also homologous to MG218 of *M. genitalium*. Like HMW2, MG218 is a terminal tip protein essential to attachment and motility (Pich et al. 2008). Along with MslA, the expression MGA267 and MGA573 were reported to vary in the Cecchini et al. study. MGA267 showed an increase in abundance in the K5234 and was also upregulated in cells grown in contact with eukaryotic cells, while MGA573 increased in abundance in K5234 but was downregulated in cells grown in contact with eukaryotic cells (Cecchini et al., 2007). The appearance of hypothetical proteins in the data set demonstrates that these proteins are expressed and presumedly functional in the two strains studied. Thirty-three percent of the *M. gallisepticum* predicted proteome is comprised of

hypothetical proteins. Functional analysis of these proteins will be essential to a comprehensive understanding of *M. gallisepticum* physiology. As demonstrated by the previous discussion, comparative functional genomics is a powerful tool and could play an important role in the investigation of proteins with no known function.

Conclusion

Using 2DE-MS based comparative expression proteomics, numerous variations between the proteomes of two genetically similar *M. gallisepticum* strains were uncovered. Strain K5234 was isolated from a flock of poultry that had been vaccinated with the live attenuated vaccine strain 6/85. Field trials demonstrated that K5234 was virulent, and that it persisted longer in birds than did 6/85. However, the two strains were indistinguishable using accepted methods of mycoplasmal differentiation (RAPD and selected sequence comparison). The nature of the phenotypic variations (increased virulence and persistence) observed during the field trials was investigated *in vitro* using 2DE-MS based proteomics. Highlights of the data set include an increased abundance in K5234 of several phase and/or antigenic variable virulence factors (to date, the only three well investigated virulence factors of *M. gallisepticum*), and a decreased abundance in K5234 of enzymes involved with pyruvate metabolism. These and other proteins in the data set could play a role in the increased virulence and persistence of K5234. They may also be involved with phenotypic variations between K5234 and 6/85 that have not been detected.

This study demonstrates the utility of quantitative comparative proteomics as a tool to investigate the molecular mechanisms behind phenomena. Regarding *M. gallisepticum*, mechanistic data could aid both the understanding of virulence at a basic level and the discovery or development of enhanced vaccine strains. As mentioned in the introduction, complications

due to *M. gallisepticum* infections are an enormous economic burden to the poultry industry (Papazisi et al., 2003). Currently, live-attenuated vaccines are the most promising options for control. Bacterins have proved ineffective. Antibiotics can control symptoms but cannot clear infections. Biosecurity measures are effective against sporadic outbreaks when flock eradication is an option. But in the egg laying industry, due to its structure and extreme size, eradication is not an option. Flocks can become infected for life, and live-attenuated vaccines are currently the best option for control (Evan et al., 2005; Gates 2008). But, as acknowledged by Jeff Evan of the USDA poultry research team, vaccine development is hindered by a lack of mechanistic knowledge concerning vaccine and field strains (the molecular studies cited in the discussion employed almost exclusively laboratory strains); what is known about field and vaccine strains is mostly phenomenological. For example, regarding the three vaccine strains currently in use, the F strain is an effective colonizer, persist well, and is capable of displacing virulent field strains, but induces mild respiratory disease and is transmissible to flocks where it is a pathogen. In contrast, strains ts-11 and 6/85 are safer and less transmissible but do not persist well and are less protective (Abd-El-Motelib and Kleven, 1993). With few exceptions, the mechanisms which account for these observations have not been investigated. If the superior protection provided by F-strain results from competitive exclusion, then what mechanisms account for its ability to out-colonize field strains and why can it achieve this exclusion better than stains ts-11 and 6/85? If F-strain's superior protection is the result of eliciting an immune response that displaces pathogens more effectively than the immune response elicited by ts-11 and 6/85, then how is this achieved? The current study is an initial (or pilot) experiment conceived to address these questions. The data generated will be used as a starting point for directed physiological and molecular experiments, hopefully resulting in a more thorough understanding of the nature of

what is desirable and undesirable in a vaccine strain. This knowledge will then be used to identify markers and develop assays with which to screen vaccine candidates or, alternatively, used as a basis for the development of recombinant vaccines.

Additionally, the potential demonstrated by this study to elucidate mechanisms of *M. gallisepticum* pathogenicity has encouraged the initiation of a long-term, large-scale research effort of which proteomics is the core approach. Currently, a LC-based proteomic comparison of K5234 and 6/85 is being carried out - which, along with the differential data generated by this study, will be used as a starting point for a large-scale systems (or modeling) project. The vaccine strains ts-11 and F-stain, the sequenced R_{low} laboratory strain, and various field strains will be incorporated into this project. The conditions under which the proteomic comparisons will be carried out will have to be standardized. However, comparative proteomics lacks the rigor of genomic and transcriptomic approaches. As mentioned in the introduction, the lack of rigor stems both from the technology and the dynamic nature of protein pools within a cell. The development of systems models for an organism that is inherently variable using technology that is inherently variable will undoubtedly be challenging and will likely require a consensus approach.

As one reviewer notes, “It is no coincidence that the first vaccines were developed against pathogens with little variability” (Telford, 2008). The complications involved with developing live-attenuated vaccines for the control of highly plastic pathogens are extensive, but a more thorough understanding of pathogenic mechanisms via global proteomic approaches will likely help address these complications. Proteomics also has the capacity to help elucidate the ill-understood genetic mechanisms that govern the replication errors that lead to phase and antigenic

variations (and the repair mechanism that overlook these errors) and also perhaps implicate environmentally responsive regulatory networks in the process.

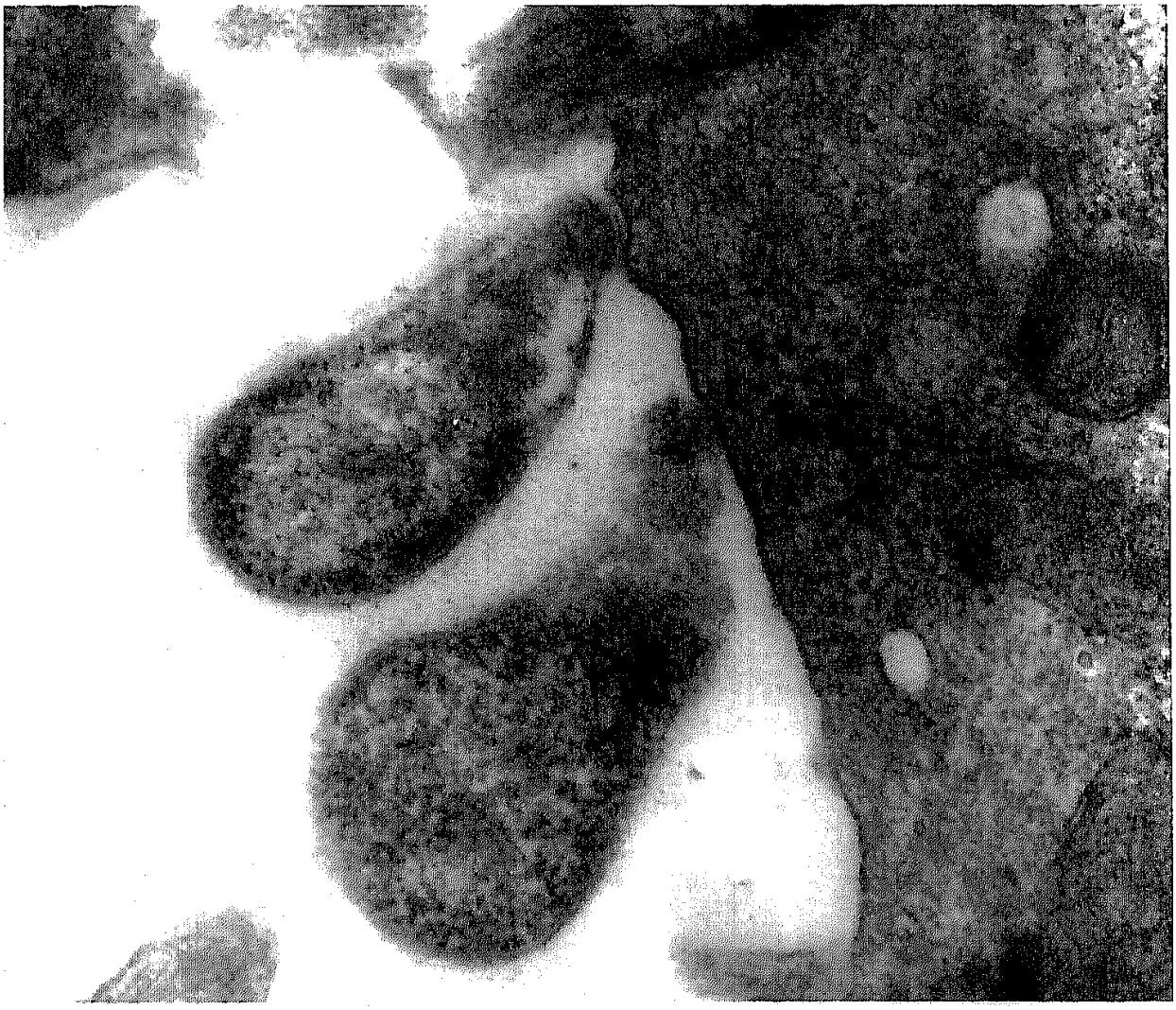

Fig. 6. Cytadherent *M. gallisepticum*. *M. gallisepticum* cells attached via attachment organelle to chick embryo epithelium 2 days post-infection (Bradbury, 2005).

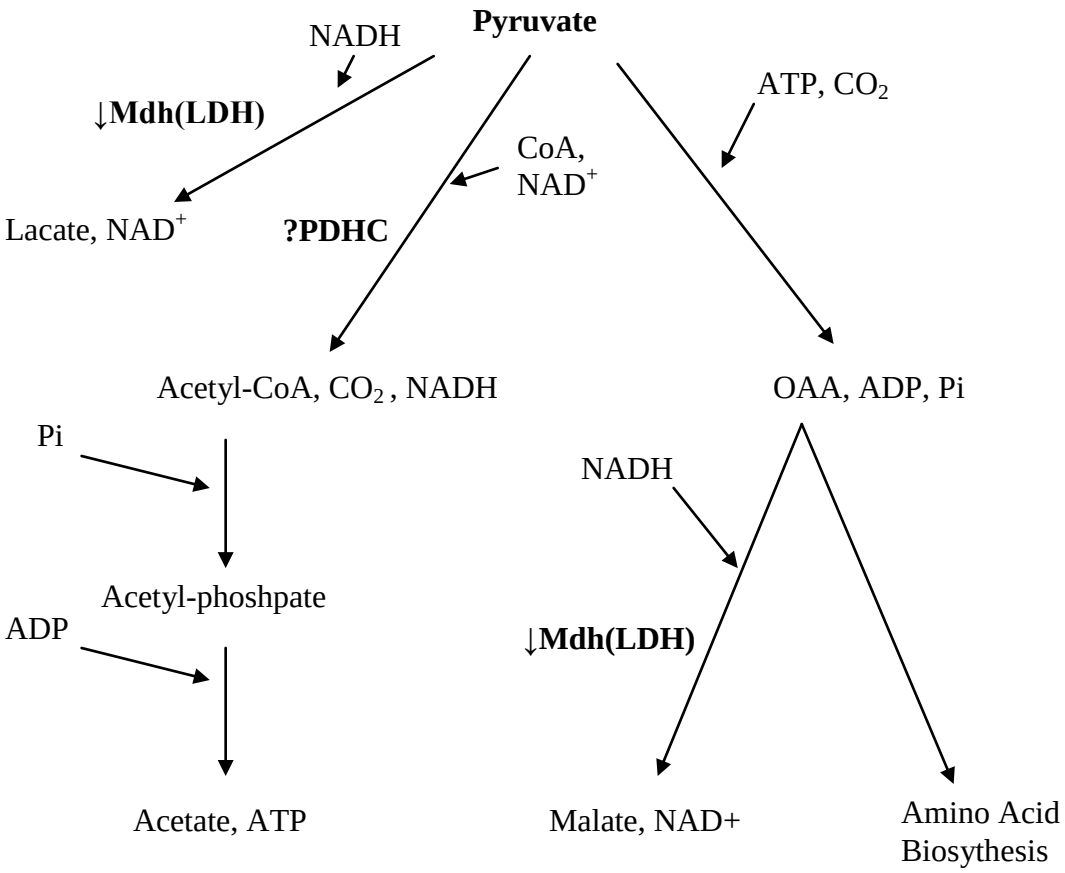

ΔMdh: -1.85, -1.71, -1.68

ΔPDHC:

AcoA: -9.13, -4.13
AceF: -1.71, -1.64
Lpd: 2.61, 2.60

Fig. 7. Pyruvate catabolism in mollicutes. This figure shows the experimental abundance changes in enzymes involved with pyruvate metabolism in the virulent K5234. Negative fold changes (Δ) indicates decreased levels in the virulent K52 strain in versus the 6/85 vaccine strain. Abbreviations: Mdh (lactate dehydrogenase), LDH (lactate dehydrogenase), PDHC (pyruvate dehydrogenase complex), AcoA (pyruvate dehydrogenase), Lpd (dihydrolipoamide dehydrogenase), AceF (dihydrolipoamide acetyltransferase).

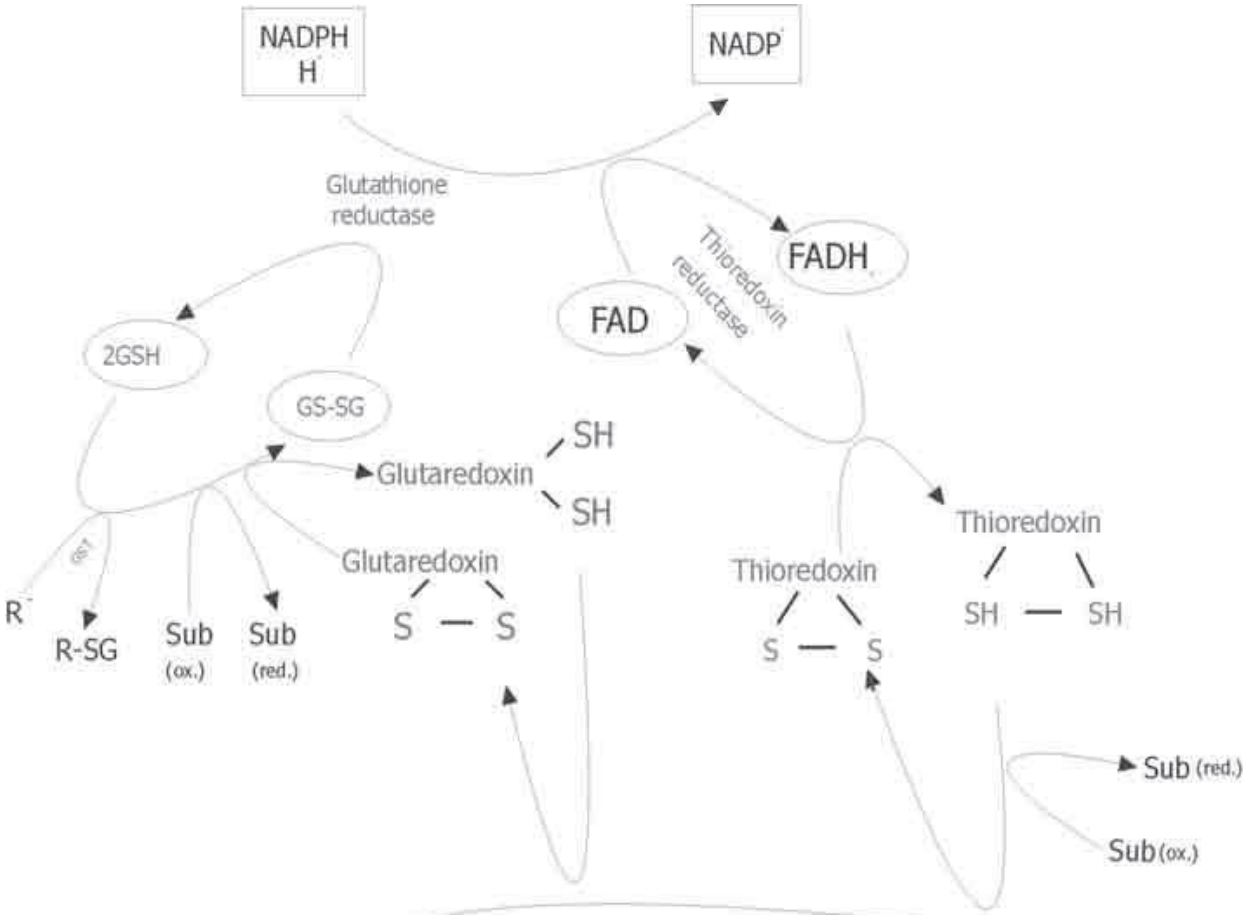

Fig. 8. $NADP^+$ / thioredoxin system (NTS).

REFERENCES

Abd-El-Motelib, T. and S. Kleven. 1993. A comparative study of *Mycoplasma gallisepticum* vaccines in young chickens. Avian Diseases **37:**981-987.

Aebersold, R. 2003. A mass spectrometric journey into protein and proteome research. J. Am Mass Spectrom. **14:**685-695.

Alban, A., S. David, L. Bjorkesten, C. Anderson, E. Sloge, S. Lewis, and I. Currie. 2003. A novel experimental design for comparative two-dimensional gel analysis: two- dimensional difference gel electrophoresis incorporating a pooled internal standard. Proteomics **3:**36-44.

Anon. 1999. Proteomics, transciptomics: what's in a name? Nature **402**:715.

Balish, F and D. Krause. 2002. Cytadherence and cytoskeleton, p. 491-518. *In* S. Razin and R. Herman (ed.), Molecular biology and pathogenicity of mycoplasmas. Kluwer Academic/Plenum Publishers, New York, N.Y.

Barre, A., A. de Daruvar, and A. Blanchard. 2004. MolliGen, a database dedicated to the comparative genomics of Mollicutes. Nucleic Acids Res. **32:**307-310.

Baseggio, N., M. Glew, P. Markham, K. Whithear, and G. Browning. 1996. Size and genomic location of the pMGA multigene family of *Mycoplasma gallisepticum*. Microbiology **142:**1429-1435.

Ben-Menachem, G., R. Himmelreich, R. Herrmann, Y. Aharonowitz, and S. Rottem. 1997. The thioredoxin reductase system of mycoplasma. Microbiology **143**:1933-1940.

Beranova-Giorgianni, S. 2003. Proteome analysis by two-dimensional gel electrophoresis and mass spectrometry: strengths and limitations. Trends Anal. Chem. **22:**273-281.

Bjellqvist, B., K. Ek, P. Righetti, E. Gianazzi, A. Gorg, R. Westermeier, and W. Postal. 1982. Isoelectric focusing in immobilized pH gradients: Principle, methodology, and some applications. J. Biochem. Biophys. Methods **6**:317-339.

Bose, S., M. Balish, and D. Krause. 2009. *Mycoplasma pneumonia* cytoskeletal protein HMW2 and the architecture of the terminal organelle. J. Bacteriol. **191:**6741-6748.

Bradbury, J. 2005. Poultry mycoplasmas: sophisticated pathogens in simple guise. Br. Poult. Sci. **46:**125-136.

Cecchini, K., T. Gorton, and S. Geary. 2007. Transcriptional response of *Mycoplasma gallisepticum* Strain R in association with eukaryotic cells. J. Bacteriol. **189:**5803-5807.

Charon, N. 2005. *Mycoplamsa* takes a walk. Proc. Natl. Acad. Sci. USA **102:**13713-13714.

Cohen, D., J. Renes, F. Bouwman, E. Zoetendal, E. Mariman, W. de Vos, and E. Vaughan. 2006. Proteomic analysis of log to stationary growth phase *Lactobacillus plantarum* cells and a 2-DE database. Proteomics **6:**6485-6493.

DeCyder Differential Analysis Software, Version 5.0. User Manual. 18-1173-16.

Evans, R. and Y. Hafez. 1992. Evaluation of *Mycoplasma gallisepticum* strain exhibiting reduced virulence for prevention and control of poultry mycoplasmosis. Avian Dis. **36:**197-201.

Evans, J., S. Leigh, S. Branton, S. Collier, G. Pharr, and S. Bearson. 2005. *Mycoplasma gallisepticum*: current and developing means to control the avian pathogen. J. Appl. Poult. Res. **14**:757-763.

Frank, S. and A. Barbour. 2006. Within-host dynamics of antigenic variation. Infect. Genet. Evol. **6:**141-146.

Gates, A., S. Frasca, A. Nyaoke, T. Gorton. L. Silbert, and S. Geary. 2008. Comparative assessment of a metabolically attenuated *Mycoplasma gallisepticum* mutant as a live vaccine for the prevention of avian respiratory mycoplasmosis. Vaccine **26**:2010-2019.

Ghaemmaghami, S., W. Huh, K. Bower, R. Howson, A. Belle, N. Dephoure, E. O'Shea, and J. Weissman. 2003. Global analysis of protein expression in yeast. Nature **425**:671-672.

Glass, J., N. Assad-Garcia, N. Alperovich, S. Yooseph, M. Lewis, M. Maruf, C. Hutchison III, H. Smith, and J. Venter. 2006. Essential genes of a minimal bacterium. Proc. Natl. Acad. Sci. USA **103:**425-430.

Glew, M., P. Markman, G. Browning, and I. Walker. 1995. Expression studies of four members of the pMGA multipgene family in *Mycoplasma gallisepticum* S6. Microbiology **141:**3005-3014.

Glew, M., N. Baseggio, P. Markham, G. Browning, and I. Walker. 1998. Expression of the pMGA gene of *Mycoplasma gallisepticum* is controlled by variation in the GAA trinucleotide repeat length within the 5' noncoding region. Infect. Immun. 66:5833-5841.

Glew, M., G. Browning, P. Markkham, and I. Walker. 2000. pMGA phenotypic variation in *Mycoplasma gallisepticum* occurs in vivo and is mediated by trinucleotide repeat variation. Infect. Immun. **68**:6027-6033.

Goh, M., T. Gorton, M. Forsyth, K. Troy, and S. Geary. 1998. Molecular and biochemical analysis of a 105 kDa *Mycoplasma gallisepticum* cytadhesin (GapA). Microbiology **144:**2971-2978.

Gorg, A., C. Obermaier, G. Boguth, A. Harder, B. Scheibe, R. Wildruber, and W. Weiss. 2000. The current state of two-dimensional electrophoresis with immobilized pH gradients. Electophoresis **21:**1037-1053

Gorg, A., W. Weiss, and M. Dunn. 2004. Current two-dimensional electrophoresis technology for proteomics. Proteomics **4:**3665-3685.

Graves, P., and T. Haystead. 2002. Molecular biologist's guide to proteomics. Microbiol. Mol. Biol. Rev. **66:**39-63.

Gutman, R., C. Berezin, R. Wollman, Y. Rosenberg, and N. Ben-Tal. 2005. QuasiMotiFinder: protein annotation by searching for evolutionarily conserved motif-like patterns. Nucleic Acids Res. **33:**255-261.

Halbedel, S., C. Hames, and J. Stulke. 2007. Regulation of carbon metabolism in the mollicutes and its relation to virulence. J. Mol. Microbiol. Biotechnol. **12:**147-154.

Hasselbring, B., J Jordan, R. Krause, and D. Krause. 2006. Terminal organelle development in the cell wall-less bacterium *Mycoplasma pneumonia*. Proc. Natl. Acad. Sci. USA **103:**16478-16483.

Henzel, W., C. Watanaba, and J. Stults. 2003. Protein identification: the origins of peptide mass fingerprinting. J. Am. Soc. Mass Spectrom. **14:**931-942.

Hudson, P., T. Gorton, L. Papazisi, K. Cecchini, S. Frasca, Jr., and S. Geary. 2006. Identification of the virulence-associated determinant, dihydrolipoamide dehydrogenase (*lpd*), in *Mycoplasma gallisepticum* through in vivo screening of transposon mutants. Infect. Immun. **74:**931-939.

Ideker, T., V. Thorsson, J. Ranish, R. Christmas, J. Buhler, J. Eng, R. Bumgarner, D. Goodlet, R. Aebersold, and L. Hood. 2001. Integrated genomic and proteomic analysis of a systematically perturbed metabolic network. Science **292**:929-934.

Jaeger, T. and L. Flohe. 2006. The thiol-based redox networks of pathogens: unexploited targets in the search for new drugs. Biofactors **27:**109-120.

Jaffe, J., N. Strange-Thomann, C. Smith, D. DeCaprio, S. Fisher, J. Butler, S. Calvo, T. Elkins, M. Fitzgerald, N. Hafez, C. Kodira, J. Major, S. Wang, J. Wilkinson, R. Nicol, C. Nusbaum, B. Birren, H. Berg, and G. Church. 2004. The complete genome and proteome of *Mycoplasma mobile*. Genome Res. **14:**1447-1461.

Jenkins, C., R. Saudrala, S. Geary, and S. Djordjevic. 2008. Structural and functional characterization of an organic hydroperoxide resistance protein from *Mycoplasma gallisepticum*. J. Bacteriol. **190**:2206-2216.

Johansson, K., and B. Pettersson. 2002. Taxonomy of mollicutes, p. 1-29. *In* S. Razin and R. Herman (ed.), Molecular biology and pathogenicity of mycoplasmas. Kluwer Academic/Plenum Publishers, New York, N.Y.

Koharyova, M. and M. Kollarova. 2008. Oxidative stress and thioredoxin system. Gen. Physiol. Biophys. **27:**71-84.

Krause, D. and M. Balish. 2001. Structure, function, and assembly of the terminal organelle of *Mycoplasma pneumoniae*. FEMS Microbio. Lett. **198**:1-7.

Lipsitch, M. and J. O'Hagan. 2007. Patterns of antigenic diversity and the mechanisms that maintain them. J. R. Soc. Interface **4**:787-802.

Liu, L., D. Payne, V. van Santen, K. Dybvig, and V. Panangala. 1998. A protein (M9) associated with monoclonal antibody-mediated agglutination of *Mycoplasma gallisepticum* is a member of the pMGA family. Infect. Immun. **66**:5570-5575.

Liu, L., K. Dybvig, V. Panangala, V. van Santen, and C. French. 2000. GAA trinucleotide repeat region regulates M9/pMGA gene expression in *Mycoplasma gallisepticum*. Infect. Immun. **68**:871-876.

Lluch-Senar, M. and Q. Pinol. 2010. Cell division in a minimal bacterium in the absence of *ftsZ*. Mol. Microbiol. **78:**278-289.

Madigan, M., J. Martinko, P. Dunlap, and D. Clark. 2009. Brock biology of microorganism, 12th ed. Pearson Benjamin Cummings, San Francisco, CA.

Maniloff, J. 2002. Phylogeny and evolution. *In* S. Razin and R. Herman (ed.), Molecular biology and pathogenicity of mycoplasmas, p. 31-45. Kluwer Academic/Plenum Publishers, New York, N.Y.

Markham, P., M. Glew, M. Brandon, I. Walker, and K. Whithear. 1992. Characterization of a major hemagglutinin protein from *Mycoplasma gallisepticum*. Infect. Immun. **60**:3885-3891.

Markham, P., M. Glew, G. Browning, K. Whithhear, and I. Walker. 1998. Expression of two members of the pMGA gene family of *Mycoplamsa gallisepticum* oscillates and is influenced by pMGA-Specific antibodies. Infect. Immun. **66**:2845-2853.

May, M., L. Papazisi, T. Gorton, and S. Geary. 2006. Identification of fibronectin-binding proteins in *Mycoplasma gallisepticum* strain R. Infect. Immun. **74:**1777-1785.

Minden, J., S Dowd, H. Meyer, and K. Stuhler. 2009. Difference gel electrophoresis. Electrophoresis **30:**S156-S161.

Much, P., F. Winner, L. Stipkovits, R. Rosengarten, and C. Citti. 2002. Mycoplasma gallisepticum: influence of cell invasiveness on the outcome of experimental infection in chickens. FEMS Immunol. Med. Microbiol. **34:**181-186.

Mudahi-Orenstein, S., S. Levisohn, S. Geary, and D. Yogev. 2003. Cytadherence-deficient mutants of *Mycoplasma gallisepticum* generated by transposon mutagenesis. Infect. Immun. **71:** 3812-3820.

Nakane, D., and M. Miyata. 2009. Cytoskeletal asymmetrical dumbbell structure of a gliding mycoplasma, *Mycoplasma gallisepticum*, revealed by negative-staining electron microscopy. J. Bacteriol. **191:**3256-3264.

O'Farrel, P. 1975. High resolution two-dimensional electrophoresis. J Biol Chem **250:**4007-4021.

O'Toole, G. 2004. Jekyll or hide?. Nature **432**: 680-681.

Pancholi, V. and G. Chhatwal. 2003. Housekeeping enzymes as virulence factors for pathogens. Int. J. Med. Microbial. **293:**391-401.

Papazisi, L., K. Troy, T. Gorton, X. Liao, and S. Geary. 2000. Analysis of cytadherence-deficient, GapA-negative *Mycoplasma gallisepticum* Strain R. Infect. Immun. **68:**6643-6649.

(a) Papazisi, L., S. Frasca Jr., M. Gladd, X. Liao, D. Yogev, and S. Geary. 2002. GapA and CrmA coexpression is essential for *Mycoplasma gallisepticum* cytadherence and virulence. Infect. Immun. **70:**6839-6845.

(b) Papazisi, L., T. Gorton, G. Kutish, P. Markham, G. Browning, D. Nguyen, S. Swartzell, A. Madan, G. Mahairas, and S. Geary. 2003. The complete genome sequence of the avian pathogen *Mycoplasma gallisepticum* strain R_{low}. Microbiology **149:**2307-2316.

Pich, O., R. Burgos, M. Ferrer Navarro, E. Querol, and J. Pinol. 2008. Role of *Mycoplasma genetalium* MG218 and MG317 cytoskeletal proteins in terminal organelle organization, gliding motility and cytadherence. Microbiology **154:**3188-3198.

Pollock, J. D. 2002. Central carbohydrate pathways: metabolic flexibility and the extra role of some "housekeeping" enzymes, p. 163-99. *In* S. Razin and R. Herman (ed.), Molecular biology and pathogenicity of mycoplasmas. Kluwer Academic/Plenum Publishers, New York, N.Y.

Pollock, J., M. Williams, and R. McElhaney. 1997. The comparative metabolism of the mollicutes (Mycoplasmas): the utility for taxonomic classification and the relationship of putative gene annotation and phylogeny to enzymatic in the smallest free-living cells. Crit. Rev. Microbiol. **23:**269-354.

Pyrowolakis, G., D. Hofmann, and R. Herrmann. 1998. The subunit b of the F_0F_1-type ATPase of the bacterium *Mycoplasma pneumoniae* is a lipoprotein. J. Biol. Chem. **273:**24792-24796.

Qu, W., Y. Zhou, C. Shao, Y. Sun, Q. Zhang, C. Chen, and J. Jia. 2009. *Helicobacter pylori* proteins response to nitric oxide stress. J. Microbiol. **47:**486-493.

Rasmussen, O., M. Shrivan, H. Margalit, C. Christiansen, and S. Rottom. 1992. Nucleotide sequence, organization and characterization of the atp genes and the encoded subunits of *Mycoplasma gallisepticum* ATPase. Biochem. J. **285:**881-888.

Razin, S., D. Yogev, and Y. Naot. 1998. Molecular biology and pathogenicity of mycoplasmas. Microbiol. Mol. Biol. Rev. **62:**1094-1156.

Rosengarten, R., C. Citti, M. Glew, A. Lischewski, M. Droesse, P. Much, F. Winner, M. Brank, and J. Sperger. 2000. Host pathogen interactions in mycoplasma pathogenesis: virulence and survival strategies of minimal prokaryotes. Int. J. Med. Microbiol. **290:**15-25.

Rottem, S. 2003. Interaction of mycoplasmas with host cells. Physiol. Rev. **83**:417-432.

Rasmussen, O., M. Shirvan, H. Margalit, and C. Christiansen. 1992. Nucleotide sequence, organization and characterization of the *atp* genes and the encoded subunits of *Mycoplasma gallisepticum* ATPase. Biochem. J. **285:**881-888.

Selinger, D., M. Wright, and G. Church. 2003. On the complete determination of biological systems. Trends. Biotechnol. **21:**251-254.

Shaw, M., and B. Riederer. 2003. Sample preparation for two-dimensional electrophoresis. Proteomics **3:**1408-1417.

Simpson, R. 2003. Proteins and proteomics: a laboratory manual. Cold Spring Harbor Laboratory Press, New York.

(a) Szczepanek, S., S. Frasca Jr., V. Scumacher, X. Liao, M. Padula, S. Djordevic, S. Geary. 2010. Identification of lipoprotein MslA as a neoteric virulence factor of *Mycoplasma gallisepticum*. Infect. Immun. **78:**3475-3483.

(b) Szczepanek, S., E. Tulman, T. Gorton, X. Liao, J. Zinski, F. Aziz, S. Frasca, Jr., G. Kutish, and S. Geary. 2010. Comparative genomic analysis of attenuated strains of *Mycoplasma gallisepticum*. Infect. Immun. **78:**1760-1771.

Tannu, N. and S. Hemby. 2006. Two-dimensional fluorescence difference gel electrophoresis for comparative proteomic profiling. Nat. Protoc. **1:**1732-1742.

Tatusov, R., D. Natale, I. Garkavtsev, T. Tatusova, U. Shankavaram, B. Rao, B. Kiryutin, M. Galperin, N. Fedorova, and E. Koonin. 2001. The COG database: new developments in phylogenetic classification of proteins from complete genomes. Nucleic Acids Res. **29:**22-28.

Telford, J. 2008. Bacterial genome variability and its impact on vaccine design. Cell Host Microbe **3:**408-415.

Throne-Steinlage, S., N. Furguson, J. Sander, M. Garcia, S. Subramanian, V. Leiting, and S. Kleven. 2003. Isolation and characterization of a 6/85-like *Mycoplasma gallisepticum* from commercial hens. Avian Dis. **47:**499-505.

Tonge, R., J. Shaw, B. Middleton, R. Rowlenson, S. Rayner, J. Young, F. Pognan, E. Hawkins, I. Currie, and M. Davison. 2001. Validation and development of fluorescence two-dimensional differential gel electrophoresis proteomic technologies. Proteomics **3:**377-396.

Unlu, M., M. Morgan, and J. Minden. 1997. Difference gel electrophoresis: a single gel method for detecting changes in protein extracts. Electrophoresis **18:**2071-2077.

van der Woude, M., and A. Baumler. 2004. Phase and antigenic variation in bacteria. Clin. Microbiol. Rev. **17**:581-611.

van der Woude, M. 2006. Re-examining the role and random nature of phase variation. FEMS Microbiol. Lett. **254**:190-197.

Venugopal, A., R. Bryk, S. Shi, K. Rhee, P. Rath, D. Schnappinger, S. Ehrt, and C. Nathan. 2011. Virulence of *Mycobacterium tuberculosis* depends on lipoamide dehydrogenase, a member of three multienzyme complexes. Cell Host & Microbe **9:**21-31.

Vogl, G., A. Plaickner, S. Szathmary, L. Stipkovits, R. Rosengarten, and M. Szostak. 2008. *Mycoplasma gallisepticum* invades chicken erythrocytes during infection. Infect. Immun. **76:**71-77.

Waites, K., and D. Talkington. 2004. *Mycoplasma pneumoniae* and its role as a human pathogen. Clin. Microbiol. Rev. **17**:697-728.

Westermeier, R. 2001. Electrophoresis in practice. Wiley-VCH, Weinheim.

Westermeier, R., and T. Naven. 2002. Proteomics in practice. Wiley-VCH, New York, N.Y.

White, D. 2000. The physiology and biochemistry of prokaryotes. Oxford University Press, Oxford, United Kingdom.

Wilkens, M., J. Sanchez, A. Gooley, R. Appel, I. Humphery-Smith, D. Horchstrasser, and K. Williams. 1996. Progress with proteome projects: why all proteins expressed by a genome should be identified and how to do it. Biotechnol. Genet. Eng. Rev. **13**:19-50.

Winner, F., I. Marková, P. Much, A. Lugmair, K. Siebert-Gulle, G. Vogl, R. Rosengarten, C. Citti. 2003. Phenotypic switching in *Mycoplasma gallisepticum* hemadsorption is governed by a high-frequency, reversible point mutation. Infect. Immun. **71:**1265-1273.

Wolf, M., T. Muller, T. Dandekar, and J. Pollack. 2004. Phylogenny of *Firmicute* with special reference to *Mycoplasma* (Mollicutes) as inferred from phosphoglycerate kinase amino acid sequence. Int. J. Syst. Evol. Mirobiol. **54**: 871-875.

Wolkenhauer, O. 2001. Systems biology: the reincarnation of systems theory applied in biology. Brief Bioinform. **2**:258-270.

APPENDIX

DEATILED LABORATORY PROTOCOLS

Crude protein extract

Lyses buffer (30 mM Tris, 7 M urea, 2 M thiourea, 4% CHAPS) – 15 ml

____make 25 ml 8 M urea, 2.3 M thiourea

____12 ml ddH_20

____12 g urea

____4.5 g thiourea

____make up to 25 ml with ddH2O

____add 250 mg amberlite and stir for 1 h

____filter into clean, rinsed bottle

____13.2 ml deionized urea/thiourea solution

____450 ul 1 M Tris

____150 ul nuclease mix

____300 ul protease inhibitor

____600 mg CHAPS

____pH to 8.6 with HCL

____make up to 15 ml

____950 ul aliquots and store at -70ºC

Protocol

1) Remove cell pellets and lysis buffer (LB) from -70ºC. Place pellets in -20ºC and allow LB to thaw at room temp.
2) Vortex LB thoroughly. Making sure all presipitated dissolves. Add required volume to pellet. Incubate at room temp for 2 min.
3) Disperse pellet by vortexing (and pipeting if needed).
4) Transfer slurry to sonication vessel incubate on ice for 10 min while:
5) Clean sonication tip with 3 rounds of ethanol and water.
6) On ice, sonicate sample 6 x 15 s on 15 s off.
7) Transfer lysate to microfuge tube and place on ice.
8) Repeat steps 1-7 for remaining samples.
9) Allow all samples to incubate at room temp for 1 hr.
10) Transfer lysates to 1.5ml thick-walled centrifuge tubes and centrifuge 40K x g at 7ºC for 1 hr.
11) Transfer clarified lysate to tube on ice.
12) Aliquot 70 ul into screw-cap tubes and store at -70ºC.

IPG strip rehydration with reswelling tray

1) Using toothbrush, clean reswelling tray with IPG detergent (or other non-ionic detergent). Rinse thoroughly with ddH20 and airdry (if needed, use crewipes to dry).
2) Remove appropriate amount of Destreak rehydration solution from -20ºC. Bottle contains 3ml of solution. 450 ul required per well. Once thawed, vortex vigorously until white solid (urea) dissolves.
3) Add IPG buffer (or other ampholytes) to 0.5% v/v (15ul to 3ml, 60ul to 6ml).

Note: Ampholyte range should match that of the strip. However, many prefer 3-11NL ampholytes when using 3-7NL or 4-7 strips.

4) For right –handed persons, orient the reswelling tray so that the acidic (+) end is to the left. Acidic end has the little circular well. Pipet 450 ul of rehydration solution into the appropriate number of wells.

   Note: Many find that applying rehydration solution toward cathodic (-) end of well results in more complete rehydration.

5) Load strips. Remove strips one at a time and load. Grasp acidic end (the one with the bar code) between thumb and index finger of left hand so that the protective cover in facing away from left hand. With right hand, gently peel off protective cover. Again with right hand, grasp basic end backing between thumb and index finger so that when the strip is flipped, the gel side is facing down and the plastic backing is up. Lower the strip so that acidic end contacts pool of rehydration buffer. Gently slide the strip back and forth across the solution, making sure that gel is wet before contacting any part of tray that is dry. Lower and release basic end so that acid end completely crosses well at acidic end.
6) Cover each strip with 3.4 ml of Drystrip cover fluid (mineral oil).
7) Insert cover, gently move tray to place of incubation, and balance with black nobs.
8) Incubate strips for 20-30 h at room temp.

Reconstitution of CyDyes

1) Transfer small volume of DMF to microfuge tube.

   Note: Once cracked, DMF reagent should only be used for 3 months. After 3 months, crack another one.

2) Remove un-opened dye from -20ºC. Leave dye in black plastic container. Incubate on ice for 5 min.
3) Add appropriate volume of DMF: 5 ul to 5mM, 10 ul to 10mM, and 25 ul to 25 mM. This gives a stock solution of 1mM.
4) Vortex dye for 30 s.
5) Spin down.
6) Immediately return dye to -20ºC.

   Note: Reconstituted dye is stable for up to 2 months or up to the expiration date.

Minimal Cy dye labeling

1) Dilute samples to 5 ug/ul (5mg/ml) with lysis buffer (LB) in a total volume of 75 ul. The LB is the diluent. This will be enough for analytical gels, several preparative gels, and a small amount to archive. To determine appropriate volume of sample and LB, divide 375ug by the concentration of the sample in ug/ul (75 ul of a 5 ug/ul solution contains 375ug). Enter the result (ul) into the chart. The left-hand blank. The one for sample. Subtract the result from 75 ul. Enter this result in the right-hand blank. The one for diluent. Label microfuge tubes according to following chart. Dilute samples. Vortex diluted samples and place on ice.

sample A (cy3 control)____		sample B (cy5 variant)____	
1A._____ul sample	_____ul diluent	1B._____ul sample	_____ul diluent
2A._____ul sample	_____ul diluent	2B._____ul sample	_____ul diluent
3A._____ul sample	_____ul diluent	3B._____ul sample	_____ul diluent
sample B (cy3 variant)____		sample A (cy5 control)____	
4B._____ul sample	_____ul diluent	4A._____ul sample	_____ul diluent

5B._____ul sample _____ul diluent 5A._____ul sample _____ul diluent

6B._____ul sample _____ul diluent 6A._____ul sample _____ul diluent

2) Transfer 55 ul of each diluted sample to single tube labeled pool. Vortex pooled sample and place on ice.
3) Multiply number of analytical gels plus one by 10 ul (6 + 1 = 7, 7 x 10 ul = 70 ul). Transfer this amount of pooled sample to tube labeled standard. This will be enough standard for each analytical gel and a little left over. Vortex standard sample and place on ice. The remaining pooled sample will be used for preparative loads and archiving.
4) Transfer 10 ul of remaining diluted sample to reaction tube (simply another microfuge tube) labeled identically to dilution tube. Place reaction tubes on ice.
5) Prepare CyDye working solution (400 pm/ul). Remove dyes from -20ºC and thaw on ice for 5 min. Keep dye tube in black plastic container. Vortex thawed dyes and spin down. Transfer small amount of DMF to tube labeled DMF. According to the following chart, transfer appropriate volume of DMF to tubes labeled Cy2, Cy3, and Cy5. Add the appropriate volume of thawed dye respected tube. Return stock dyes to -20ºC immediately. Vortex diluted dye, spin down, and place on ice in the dark.

    4 samples: add 2 ul stock to 3ul DMF

    6 samples: add 3 ul stock to 4.5ul DMF

    8 samples: add 3.5 ul stock to 5.25ul DMF

6) Reaction. Working methodically, add 1ul Cy3 to Cy3 reaction tubes. Vortex each for 10 s, spin down, and return to ice. Add 1ul Cy5 to Cy5 sample tubes. Vortex each for 10 s, spin down, and return to ice. Add 1 ul Cy2 per 10 ul standard sample to standard reaction tube. Vortex, spin, and return to ice.

7) Incubate reaction tubes for 30 min on ice protected from light. Place 10 mM lysine on ice.
8) Quench reaction. Add 1 ul 10 mM lysine to Cy3 and Cy5 reaction tubes. Add same volume of 10 mM lysine to standard reaction tube that was used for Cy2 in step 6. Vortex and spin down each sample before return to ice protected from light.
9) Incubate reaction tubes for 10 min.
10) Proceed to reduction and 1st dimension or store samples at -70ºC.

Reduction and 1st dimension

1) Remove aliquot of 2X solubilization buffer (2XSB), aliquot of rehydration buffer (RB), CyDye labeled samples, and pooled sample from -70ºC. Once thawed, vortex each. Ensure precipitates are dissolved. Spin down labeled samples.
2) For each sample set, marry Cy3 and Cy5 samples by transferring entire contents of Cy5 tubes to Cy3 tubes.
3) Add 12 ul standard sample to each Cy3 tube. Now each Cy3 tube should contain 36 ul.
4) Add 36 ul 2XSB to each sample and vortex.
5) Transfer amount of pooled sample needed for preparative gels to fresh tube. Add equal volume of 2XSB and vortex.
6) Incubate samples on ice in the dark for 30 min while:
7) Using treezers, gasp the strip's basic end backing. Lift, flip, and place in ceramic boat so that acidic end (the one with the + and barcode) is pointed toward end of boat and cathodic end of gel is at square end of boat. Make sure gel surface is up.
8) Cover each rehydrated strip with 4.4 ml Drystrip cover fluid (mineral oil).

9) Place electrode pads moistened with 150 ul ddH_20 on cathodic and acidic end on gel, not the gel backing.
10) Place electrodes on electrode pads, several mm from the ends of the gel. Ensure that the electrode is over the gel, not the gel backing.
11) Place sample cup several mm from the acidic end electrode pad. Ensure that the cut feet contact the bottom of the boat and that they do not contact the boat's guides. Observe at eyes level to make sure.
12) Fill each sample cup with 100 ul of Drystrip cover fluid. Allow gels to sit for 10 min while:
13) Add 28 ul RB to each reduced sample (total volume now 100ul).Brig preparative sample up to 100 ul with RB. Vortex each and spin down.
14) Ensure that cups are not leaking by making sure that level of Drystrip cover fluid in each cup has not dropped.
15) Add entire sample contents (100 ul) to sample cup.
16) Place strips on IEF platform. Ensure that boat electrodes contact platform electrodes (the gold part).
17) Place covers over boats and close hood.
18) Toggle to or program desired protocol, press start, enter the number of gels, and press start again.
19) Protect unit from light.
20) Return remaining pooled sample to -70ºC.
21) After run completed, store strips in capped plastic tubes or proceed directly to strip equilibration and 2^{nd} dimension.

Casting analytical and preparative gels

1) Prepare bind silane solution. The plates with vinyl spacers will be the back plates of sandwiches. Gels are bound to the back plates. 4ml bind solution needed per back plate.

   Bind–silane working solution (prepare fresh) – 10ml (enough for 2 back plates)

   ____8 ml 200 proof ethanol

   ____1.8 ml ddH_2O

   ____200 ul glacial acetic acid

   ____12.5 ul bind-silane (this is 2X recommended amount)

2) Treat plates. Plates should have been cleaned and then treated with 1% HCL. Plates should be dry and free of dust. Place plates on crewipes so that vinyl spacers are up. This will be the inside of the gel sandwich. Pipet 4 ml of bind solution onto plates. Thoroughly spread solution over plates with crewipe (or other lint-free wipe). Work up and down across plates and across plates up and down. Cover plates with crewipes to protect from dust. Allow plates to sit for 45 min while:

3) Prepare gels solution. Leave out APS. Measure larger volumes with 100ml graduated cylinder.

   Gel solution (12.5%) – 940 ml

   ____294 ml 40% monomer solution

   ____235 ml 1.5M TrisCl pH8.8

   ____392 ml ddH2O

   ____9.4 ml 10% SDS

   ____376 ul TEMED (80% of recommended amount)

4) Prepare displacing solution.

   Displacing solution (0.375 M TrisCl pH 8.8, 50% glycerol, 0.002% bromophenol blue) – 120ml

   ____20 ml ddH_20

   ____30 ml 1.5M TrisCl, pH 8.8

   ____70 ml glycerol

   ____240ul 1% bromophenol blue

5) Prepare 10% APS by adding 1 g of APS to 9.6 ml ddH2O.

6) After 45 min (step 2), place reference markers on plates. Place reference markers 10.5 cm up from plate bottoms (vinyl spacers go all the way to the edge at the bottom of the plates) and slightly inward (several mm) of the vinyl spacers. Use tweezers to place markers and press marker hard to plates. Allow plates to sit for additional 45 min before loading the caster.

7) Grease gasket on removable front face of caster.

8) Load caster. Work briskly. Place plastic separator sheet to back of caster. Then back plate (one with spacers). Then front plate. Then thin separator sheet, etc. Ensure all plates are flush to one side of caster and all plate bottoms are flush and seated on caster bottom. When all plates are loaded, fill any space between last plate and front of caster with thin or thick separator sheets so that final sheet is flush with the front of the caster.

9) Secure front face of the caster.

10) Level caster.

11) Secure funnel tube stem in displacing solution reservoir.

12) Fill reservoir with 85 ml displacing solution.

13) Add 9.4 ml 10% APS to gel solution and gently mix.
14) Pour gel solution until level with mark 3 cm from top of front plates and stop flow.
15) Remove funnel stem.
16) Adjust solution level by adding needed amount of remaining displacing solution to reservoir.
17) Overlay gels with 2 ml water-saturated butanol.
18) Allow gels to sit for at least 1.5 h.
19) Place caster in large autoclave bucket and dismantle from plate.
20) Remove plates. Rinse plate with ddH_2O. Rinse top of gel sandwiches, making sure water saturated butanol is displaced. Trim off excess polymer.
21) Lay plate on seal wrap. Fill top gel gaps with storage buffer. Pipet storage buffer along the gel sandwich bottoms. Wrap sandwiches.
22) Store overnight at room temperature.
23) If 2nd dimesion not started day after casting, gels can be stored for several days at 4ºC.

Equilibration and 2nd dimesion

1) Remove equilibration buffer (EB) from -4ºC. 1 tube (50 ml) per gel.
2) Split EB between 2 flasks. Add 0.5% DTT to one and 4.5% iodoacetamide to the other.

_____ml EB x 0.005 = _____g DTT

x 0.045 = _____g iodo

3) Stir flask while:
4) Turn on heating block. Insert required aliquots (1 per gel) of agarose sealing solution.
5) Dilute electrophoresis buffer and pre-chill if desired.
6) Remove strip tubes from -70Cº. Incubate at room temp for 10 min in dark

7) Add 20 ml DTT EB to gel tubes. Cap tubes and place on shaker at 80rpm. Incubate 15min in dark while:
8) Rinse gel sandwiches with ddH_2O. Invert sandwiches and place in plate rack while:
9) Pour off DTT EB.
10) Add 20 ml ioda EB to gel tubes. Cap and shake as before. Incubate 10min in dark
11) Drain EB.
12) Fill 100 ml cylinder with 1X electrophoresis buffer.
13) With clean forcepts remove strip from tube and rinse in 100 ml cylinder containg electrophoresis buffer.
14) Lay strip on ledge at top of sandwich gel with the acidic end to the left.
15) Use clean rule to position IEF strip on top of 2^{nd} dimension gel. Make sure ruler only contacts IEF strip gel backing.
16) Cover IEF strip with 1ml agarose sealing solution.
17) Incubate sandwiches for 5 min to allow sealing solution to solidify while:
18) Set tank to circulate. Add electrophoresis buffer to gel tank.
19) Insert appropriate number of gel blanks.
20) Ensure agarose sealing solution is solid.
21) Insert sandwiches into gel tank.
22) Program desire protocol and start.
23) After run, remove and rinse gel sandwiches with ddH_2O.
24) Remove front plate from preparative gels. Place gels in fixing solution and store in dark.
25) Wrap analytical gels in seal wrap. Protect from light. Scan immediately.

Deep Purple Staining

Solutions

Fixing solution (7.5% acetic acid / 10% methanol) – 1 L

____825 ml ddH2O

____75 ml glacial acetic acid

____100 ml methanol

Wash solution (35 mM NaHCO3 / 300 mM Na2CO3) – 1 L

____750 ml ddH2O

____2.94 g NaHCO3

____31.8 g Na2CO3

____make up to 1 L

____verify pH 10 – 11 (solution can be stored up to 2 weeks)

Working stain solution – 500 ml/gel – 500 ml

____remove stain from -20ºC and incubate at room temp for 2 min

____shake concentrate briefly and transfer 2.5 ml to 500 ml ddH_2O

Stabilization solution (7.5% acetic acid) – 3 L

____2775 ml ddH_20

____225 ml glacial acetic acid

Protocol

1) Thoroughly clean and rinse (ddH_2O) staining containers.
2) Prepare fixing solution.

3) Remove gels from electrophoresis tank. Remove top plate. Place gels in 1 L of fixing solution and incubate overnight.
4) Remove gel, rinse container and wash gel in 1 L wash solution for 30 min at 25 rpm.
5) Remove gel, rinse container and incubate in 1 L ddH_2O for 5min at 25 rpm.
6) While gel is incubating in water, make working stain solution.
7) Remove gel, rinse container and cover each gel with 500 ml working solution. Incubate for 1 h with gentle agitation (40 rpm) **protected from light.**
8) Remove gel, rinse container, and place gel in 1 L stabilization solution with gentle agitation **protected from light** for at least 20 min.
9) Repeat step 8 twice (optional).
10) Scan gel using the green laser (532nm) and emission filter 560LP (PMT voltage will have to be adjusted according to the protein load if saturation is an issue. Start with 550. Do not go above 600). Or gels can be stored at 4ºC, between glass plates, in the dark, in stabilization solution or 0.75% acetic acid.

Sypro Ruby staining

Solutions

Fixing solution (7.5% acetic acid / 10% methanol) – 1 L

____825 ml ddH_2O

____75 ml acetic acid

____100 ml methanol

Stabilization solution (7.5% acetic acid) – 3L

____2775 ml ddH_20

____225 ml glacial acetic acid

Protocol

1) Thoroughly clean and rinse (ddH_2O) staining containers.
2) Remove gels from electrophoresis tank. Remove front plate. Place gels in 1 L of fixing solution and incubate overnight.
3) Remove gel, pour out fixing solution, rinse container, then fill with 400 ml Sypro Ruby, and insert gel. Incubate with gentle shaking (50rpm) overnight protected from light.
4) Wash gels 6 x 20 min with 1.2L ddH_20 with shaking at 25 rpm protected from light. Rinse container between each wash. Alternatively, transfer gel from stain to 100% methanol for exactly 1.00000 min (use stop watch). Wash gel with ddH_20 and scan.
5) Scan gel with Sypro Ruby emission filter.
6) Replace front glass and store in stabilization solution.

Scanning analytical gels

1) Remove gels from tank, rinse with ddH_2O, and wrap with sealwrap.
2) Wrap all seal wrapped gels in foil to protect from light and place at -4ºC.
3) Remove 1 gel. Rinse with ddH_2O, Dry with crewipe while:
4) Using crewipe, clean scanner window with 2 rounds of 100% ethanol followed by ddH_2O.
5) Place position bar on window on edge closest to user.
6) Ensure that window is completely dry and position gel. Orient gel so that the top plate is up and ledge is left. Position acidic side of gel on metal tabs of positioning bar.
7) Grasp basic side of gel with small positoning bar and lower gel. Close scanner hood.
8) Open **Scanner Control**.

9) Set **Acquisition Mode** to **Fluorescence**.

10) Click **Setup**

11) On **Typhoon Scanner Control** under column **Use** de-select image **2**, **3**, and **4**.

12) Set **Emission filter** to **520 BP 40 CY2, Blue FAM**.

13) Ensure **Laser** is **Blue2 (488)** and **Sensitivity** is **Normal**.

14) Set **PMT** voltage to **550**.

15) Under **Auto Link Mode** select **Sensitivity**.

16) Select **OK**.

17) On **Typhoon Scanner Control** tick **Press Sample**.

18) Set **Pixel size** to **1000 microns**.

19) Select **SCAN**.

20) On **Multiple Sample Naming** screen select **SCAN**

21) Watch real time display of scan.

- If red spots appear on gel return to **Fluorescent Setup for Typhoon9410** screen. Reduce **PMT** voltage by 10 units (to 540) and repeat pre-scan. Repeat until no red spots. Subract 10 units from the final PMT voltage that produces no red spots. This will be the PMT voltage for Cy2.
- If no red spots appear on gel, increase PMT voltage by 10 units (560) and scan. Repeat until 1 or 2 red spots appear. Subtract 15 units from this voltage. This will be the voltage for Cy2.

22) Repeat steps 10-21 for Cy3 and Cy5.

23) Go to **Fluorescent Setup for Typhoon 9410** screen. Under **Use** select **Image 1, 2,** and **3**.

24) Set image 1 to **520 BP 40 CY2, Blue FAM**. Set image 2 to **580 BP 30 Cy3, TAMRA, AlexaFlour 546**. Set image 3 to **670 BP 30 Cy5**.
25) Enter respected voltages under **PMT**.
26) Ensure **Laser** for image 1 is **Blue2 (488)**, for image 2 is **Green (532)**, and for image 3 is **Red (633)**.
27) **Sensitivity** for all should be **normal.**
28) Ensure **Auto Link Mode** is **Sensitivity**.
29) Select **OK**.
30) On **Typhoon Scanner Control** window, under **Tray,** select **DIGE Ettan Dalt** and number **1**.
31) Under options, tick **Press Sample**. Set **Pixel size** to **100 microns**. Set **Focal Plane** to **+3 mm**.
32) Tick **DIGE File Naming Format** and select **SCAN**.
33) On **Multiple Sample Naming** screen in **Use Common Settings for All samples** box on line **Folder**, **Browse** to desired folder for data output and select **Set.**
34) On line **Base File Name**, enter the experiment name and the gel being scanned and select **SCAN**
35) After scan complete open **ImageQuant** software. Under **Tools**, select **Define area of Interest**. Outline desired area of interest.
36) Under **File**, select **Save Gel Files from Dataset to Folder.**
37) Select desired folder and **Save.**

.tiff or .gel files and can now be opened with DeCyder.

Scanning preparative gels

1) Using crewipe, clean scanner window with 3 rounds of 100% ethanol followed by ddH_2O.
2) Place clean and dust-free top plate on gel adhered to back plate. Lower at an angle to prevent trapping air.
3) Allow gel sandwich to sit for 5 min.
4) Remove gel sandwich from stabilization solution. Rinse with ddH_2O. Dry with crewipe.
5) Position gel on window as per steps 5-7 of **Scanning analytical gels**.
6) Optimize PMT voltage as per steps 14-21 of **Scanning analytical gels**.
7) Scan gel as per step analytical gels, using the manufacturer's recommended parameters.
8) Store gel sandwich in stabilization solution at 4ºC.

Decyder differential analysis (overview)

1) Open Decyder module **DIA** / Create file for .gel file of analytical gel / Process gel image (establishes spot boundaries) / filter / Save as .dia file and export as .xml file / repeat for remaining analytical gels
2) Open Decyder module **BVA** / Import .xml files of all analytical gels / Assign gel functions / establish experimental groups / In Match Table screen, merge spots and landmark / Match / Run student's T-test / Filter data / Confirm results

Plate cleaning and hydrolysis of residual bind silane

1) Dissemble gel sandwich. Place top plate aside in plate rack. Use plastic wedge to remove bulk polymer from back plate. Work up and down and across plate.
2) Soak back plate in 1% Contrad for 2 h.
3) Scrape plate as per step 1. Rinse plate thoroughly to remove non-adhered polymer. Using plastic wool, scrub plate thoroughly, rinse again, and dry with crewipe.
4) Inspect plate for residual polymer. Repeat step 3 until all polymer is removed.
5) Soak plates in 1% HCL for 2 h.
6) Rinse plates thoroughly with ddH_2O.
7) Place plates in plate rack and set aside to dry. Put plate rack in autoclave bag labeled. **Do Not Autoclave**.

Spot picking

1) Remove gel tray from spot picker and rinse with ddH_20.
2) Cover the surface of the tray with ddH2O (just enough to cover bottom of tray).
3) Remove gel from 4ºC. Gently remove top plate. Orient try so that corner feet are toward user. Place plate in tray, oriented so that bottom of gel is toward user. Secure gel. Making sure both reference markers are between white lines of tray. Place tray with gel in picker. Bottom corner feet fit on knobs toward user. Make sure all 4 feet are fit onto knobs.
4) Rinse 96-well plate with ddH2O. Place in bottom left (**A**) plate position. Situate down and to the left.
5) Remove camera cover.
6) Close cabinet.
7) Place feed tube in bottle of ddH_2O.

8) Open **Ettan Spot Picker**.
9) Click **Tools** then **Prime Syringe**. Enter **20** then click **Prime**.
10) Set **Z-height.**
11) Bottom right screen, click **Load Pick List** and open text file pick list.
12) Click **Skip** in **Scanner Correction** box.
13) After spots appear, click **Next** at bottom right. Read message and click **Next** again.
14) Click **Auto Detection** in **Detect Marker** box.
15) When marker detection complete, click **next** and enter output directory file name and route. Then click **Create Directory**.
16) Click **Run batch**.
17) When picking complete, confirm plugs in each well by removing ddH2O and inspecting well. Alternatively, scan 96-well plate with Deep Purple protocol. The gel can also be re-scanned.
18) Replace cap on camera. Remove gel try. Remove gel from tray. Rinse tray and leave inverted to dry.

Protein digestion

Reagent prep (20 samples)

50mM ammonia bicarb / 50% acetonitrile – 8 ml

____4 ml ddH_2O

____4 ml acetonitrile

____31 mg ammonium bicarb

75% acetonitrile – 4 ml

____3 ml acetonitrile

____1 ml ddH_2O

20 ug/ml trypsin / 20 mM ammonium bicarb – 1 ml

____ to 10 ml ddH_2O, add 16 mg ammonium bicarbonate (20 mM)

____add 1 ml 20 mM ammonium bicarbonate to trypsin vial (20 ug)

____mix and transfer to tube

50% acetonitrile / 0.1% TFA – 4 ml

____2 ml ddH_2O

____2 ml acetonitrile

____4 ul TFA

Protocol

1) Prepare first 3 reagents…keep reconstituted trypsin at 4ºC.
2) Remove ddH_2O, making sure not to smash or loose the plugs.
3) Add 100 ul 50mM ammonium bicarbonate/50% acetonitrile / incubate 20 min / remove solution.
4) Repeat.
5) Add 100 ul 75% acetonitrile / incubate 20 min / remove solution.
6) Dry plugs in speed vac (may need to remove rotor) for 30 min with no heat.
7) Add 7 ul 20 ug/ml trypsin directly to each plug.
8) Seal plate and incubate at 37ºC overnight.
9) Make up last reagent.
10) Add 60 ul 50% acetonitrile/0.1% TFA / incubate 20 min / transfer to fresh tube.

11) Add 40 ul 50% acetonitrile/0.1% TFA to each well / incubate for 20 min / marry to previous 60 ul.
12) Dry solution in speedvac (no heat) until dry…around 2 h.
13) Proceed to ziptip or freeze samples at -20ºC.

Target plate cleaning

1) Cover plate surface with target plate cleaning solution.
2) Scrub surface with toothbrush.
3) Rinse scrubbed plate with ddH_2O.
4) Dry plate with crewipe.
5) Dab very small amount of Pol metal cleaning polish on fresh crewipe.
6) Polish plate with crewipes in circular motion until no black residue is seen on the crewipes (**do not let polish dry**).
7) Rinse plate with isopropanol and allow to air dry.

De-salting (uC18) for MS

Wetting solution (50% ACN in milli-Q water) – 1 ml

____500 ul ddH_2O

____500 ul ACN

0.1% TFA in milli-Q water – 1 ml

____1 ml ddH20

____1 ul TFA

Elution solution (0.1% TFA / 70 % ACN in milli-Q water) – 1 ml

____700 ul ACN

____300 ul ddH_2O

____1 ul TFA

Protocol

1) Add 1.5 ul neat formic acid and vortex.
2) Add 8.5 ul 0.1% TFA, vortex, and spin down.
3) At max volume setting (10 ul) aspirate and discard wetting solution twice.
4) Equilibrate by aspirating and discarding 0.1% TFA 10X.
5) Bind by aspirating and dispensing sample 7X.
6) Wash bound sample 10X with 0.1% TFA.
7) Aspirate and elute 0.7 ul elution solution 5X (no air) and spot sample directly onto TOF/TOF plate.
8) Allow to dry (or almost dry) and spot .3 ul alpha matrix onto each spot.
9) Keep plate in dark until processing.